CHAIR OF THERMAL PROCESSING TECHNOLOGY
Head of Chair:
Univ.Prof. Dipl.Ing. Dr.techn. Harald Raupenstrauch
Montanuniversitaet Leoben
Franz-Josef-Strasse 18
A-8700 Leoben
www.unileoben.ac.at

Master Thesis

Numerical Investigation of the Interaction between Dust Explosions and Inert Particulate Additives Using an Euler-Lagrangian Approach in OpenFOAM ®

created at the

Chair of Thermal Processing Technology

Submitted by:
Stefanie Tomasch BSc.
1035289

Supervisors:
Univ.Prof., Dipl.-Ing., Dr.techn. Harald Raupenstrauch
Ass.Prof., Dipl. Ing., Dr.mont. Hannes Kern
DDipl. Ing. Werner Pollhammer

Leoben, November 12, 2016

EIDESSTATTLICHE ERKLÄRUNG

Ich erkläre an Eides statt, dass ich diese Arbeit selbstständig verfasst, andere als die angegebenen Quellen und Hilfsmittel nicht benutzt und mich auch sonst keiner unerlaubten Hilfsmittel bedient habe.

AFFIDAVIT

I declare in lieu of oath, that I wrote this thesis and performed the associated research myself, using only literature cited in this volume.

Date

Signature

Danksagung

Ich hoffe durch das Verfassen dieser Arbeit mehrere Monate interessante und lehrreiche Forschung an einem Thema das mich sehr begeistert bestmöglich festgehalten zu haben. Ich hatte das Glück, in dieser Zeit sehr große Unterstützung zu bekommen in fachlicher wie auch in menschlicher Hinsicht.

Zu allererst möchte ich mich bei Herrn Univ.Prof., Dipl.-Ing., Dr.techn. Harald Raupenstrauch bedanken der es mir ermöglicht hat, meine Masterarbeit am Lehrstuhl für Thermoprozesstechnik zu schreiben. Auch möchte ich allen Mitarbeitern des Lehrstuhls für die nette Aufnahme, die tolle Arbeitsatmosphäre und die schöne Zeit danken.

Frau Dipl.-Ing. Katja Hüttenbrenner und Herrn Ass. Prof., Dipl.-Ing., Dr.mont. Hannes Kern gilt mein Dank für ihre fachliche Unterstützung im Bereich Anlagensicherheit und Explosionsschutz sowie für ihre Hilfe bei allen organisatorischen Angelegenheiten durch die ich mich voll und ganz der Aufgabenstellung widmen konnte.

Ein besonderer Dank gilt Herrn DDipl.-Ing. Werner Pollhammer, der nicht nur ein toller Kollege, sondern auch ein hervorragender Betreuer ist und dessen kreative Problemlösungsstrategien mir immer wieder sehr geholfen haben. Herrn Dipl.-Ing., Dr.mont. Christoph Spijker danke ich für die Unterstützung in besonders kniffligen Situationen, in denen sein umfangreiches Wissen und seine Erfahrung gefragt waren. Allen Vieren danke ich für den Freiraum, den ich bei der Gestaltung der Arbeit hatte und die Freude, mit der sie selbst an diesem Thema forschen. Diese hat mich bei so manchem Rückschlag wieder neu motiviert.

Ein großer Dank gilt auch meiner Familie, allen voran meinen Eltern Manfred und Daniela Tomasch, die mir immer geholfen haben alle meine Ziele zu erreichen und eine große Stütze für mich sind. Meiner Schwester Melanie möchte ich für die schöne Studienzeit mit ihr danken und dafür, dass durch sie Leoben auch immer ein wenig zu Hause für mich war. Herrn Felix Gstrein danke ich dafür, dass er es versteht meine Zweifel und Rückschläge ins rechte Licht zu rücken und mich auf jegliche Art zu unterstützen weiß.

All meinen Freunden und Studienkollegen möchte ich abschließend noch dafür danken, dass ich trotz der arbeitsintensiven Zeit auch auf viele schöne Momente mit ihnen zurückblicken kann.

Glück Auf!

Abstract

The occurrence of dust explosions in industry is still a serious threat to plants across all types of applications and should not be underestimated. Besides its own destructive effects the propagation of dust explosions through the plant can indirectly cause other dangerous failures. Extinguishing barriers proved to be a very successful countermeasure to prevent this. The fundamental mechanisms that are responsible for the effective intervention of the material into the combustion process is still subject of research. A reason for the very little knowledge about this topic is that most related processes take place within a few milliseconds and are difficult to record in laboratory experiments.

The aim of this thesis was to elucidate the influence of particulate additives on the ignition and flame propagation behaviour in lycopodium/air mixtures using Computational Fluid Dynamics. For this purpose an Euler-Lagrangian approach was used. For a better comparability the geometries were derived from the associated test apparatus with which related experiments are carried out at the Chair of Thermal Processing Technology. Concerning the choice of additives it was aimed to represent a broad range of different extinguishing materials with varying response to heat input. Thereby the focus was placed solely on thermal effects. The three extinguishing agents that were used for this purpose are simple inert particles that can only absorb heat according to their thermal capacity, water-laden particles with the ability to evaporate and solid particles that show a simplified melting process. Besides getting a more comprehensive insight into the interaction between flammable dust/air mixtures and particulate additives, the determination of the necessary Ignition Energy and the Flame Propagation Velocity for each set-up was also part of this work.

Kurzfassung

Das Auftreten von Staubexplosionen stellt für die Industrie nach wie vor ein ernsthaftes, nicht zu unterschätzendes Risiko dar und betrifft Anlagen in unterschiedlichsten Einsatzgebieten. Neben den direkten Folgen am Entstehungsort birgt die Ausbreitung von Staubexplosionen auf benachbarte Anlagenteile die Gefahr, indirekt weitere Störfälle auszulösen. Löschmittelsperren aus partikulärem Feststoff haben sich in diesem Zusammenhang in der Praxis als erfolgreiche Gegenmaßnahme erwiesen. Die fundamentalen Mechanismen, die der Wirksamkeit dieser Methode zu Grunde liegen, sind jedoch noch wenig bekannt. Ein Grund dafür ist, dass alleine durch Experimente viele Effekte, deren Auftreten im Bereich weniger Millisekunden liegt, nicht ausreichend erfasst werden können.

Ziel dieser Arbeit war es mittels computerunterstützter numerischer Strömungssmechanik (CFD) die Einflüsse unterschiedlicher partikulärer Feststoffe auf die mindestens notwenige Zündenergie sowie die Flammenausbreitung in einem Lykopodium/Luft-Gemisch zu untersuchen. Zum Einsatz kam dafür die Euler-Lagrange Methode. Zur besseren Vergleichbarkeit wurden die verwendeten Geometrien in Anlehnung an die Versuchsapparate am Lehrstuhl für Thermoprozesstechnik gestaltet. Bezüglich der Zugabematerialien war es das Ziel, ein möglichst breites Spektrum an infrage kommenden Löschsubstanzen zu erfassen, die jeweils unterschiedlich auf Erwärmung reagieren. Die Arbeit konzentrierte sich dabei ausschließlich auf auftretende thermische Wechselwirkungen. Es wurden zum einen Partikel gewählt, welche nur aufgrund ihrer Wärmekapazität thermische Energie aufnehmen sowie zum anderen wasserbeladene und niedrig schmelzende Feststoffpartikel. Neben Erkenntnissen bezüglich der Wechselwirkung von Additiven mit den gezündeten Staub/Luft-Gemischen sollten auch die Flammenfortpflanzungsgeschwindigkeit und die notwendige Zündenergie für alle betrachteten Systeme ermittelt werden.

Contents

Formula symbols

A	Area	$[m^2]$
d	Diameter	$[m]$
E	Energy	$[J]$
g	Acceleration of Gravity	$[m/s^2]$
H / h	(Specific) Enthalpy	$[J/kg]/[J]$
K	Mechanical Energy	$[J]$
k	Kinetic Turbulent Energy	$[J]$
m	Mass	$[kg]$
p	pressure	$[Pa]$
q / Q	(Specific) Heat	$[J]$
t	Time	$[s]$
T	Temperature	$[K]$
u	Inner Energy	$[J]$
U	Velocity	$[m/s]$
V	Volume	$[m^3]$
Y	Mass Fraction	$[-]$
α	Heat Transfer Coefficient	$[W/m^2K]$
ϵ	Turbulent Dissipation	$[J]$
λ	Thermal Conductivity	$[W/mK]$
μ_t	Eddy Viscosity	$[Pas]$
κ	Mixing Parameter	$[-]$
ρ	Density	$[kg/m^3]$
σ	Stress	$[Pa]$
σ	Standard Deviation	

Acronyms

TPT	Chair of Thermal Processing Technology
CFD	Computational Fluid Dynamics
CCD	Charge-coupled Device
FPS	Flame Propagation Velocity
CSV	Comma Separated Value

List of Figures

List of Tables

1 Introduction

1.1 Problem Statement

At the chair of Thermal Processing Technology at the University of Leoben a main focus in research activity is placed on industrial plant and process safety. One main issue in this extensive scientific field constitutes the investigation of dust explosions. Their occurrence in industry is still a serious risk for lives, health and property and affects plants across all types of branches dealing with flammable particulate matter in any kind of way. Therefore, it is essential to find new possibilities to reduce the risk of occurrence and yet minimize negative effects in case of an explosion.

Many safety devices that are nowadays in use for explosion suppression or extinction are proved to be successful by experimental tests with only little knowledge about their fundamental functional principles. Important mechanisms in dust, air and extinguishing medium containing mixtures that are decisive for the explosion progress occur within a few milliseconds. Therefore it is challenging to identify them only experimentally.

1.2 Objective

The aim of this Master thesis was to gain a better understanding of the impact different types of non-flammable finely dispersed additives have on dust explosion initialisation and propagation. For this purpose a CFD-based model with an Euler-Lagrangian approach was used to simulate the spark ignition and explosion proceeding in a lycopodium/air mixture with different particulate additives varying in their concentration, grain size and physical properties. Several case studies should give a better insight into the mechanisms that can influence the behaviour of dust explosions and for experimental evaluation of the results the minimal necessary ignition energy was determined for each set-up as well as the Flame Propagation Speed.

1.3 Methodological Approach

This Master thesis supplements a previous work done on this topic. Therefore basic case set-up, geometry and choice of solver were taken from Pollhammer [1] with slight changes of material properties and adaptations necessary for compatibility with OpenFOAM® 2.4.0. At the beginning the present solver was modified in order to be able to write out all source terms of the energy conservation equation for the Eulerian phase. The first studies were run with inert particles, subsequently they were replaced by water-laden particles and the last cases were simulated with finely dispersed melting additives. The gathered results could then be compared against experimental data, whereby the focus did not lie on the verification of one or the other but on approaching a scientific problem with different methods that are complementary.

2 Literature Review

2.1 General Aspects of Explosion Protection

For a dust explosion to occur, several conditions coincidently have to be met. The absence of only one of these requirements prohibits the explosion. Analogous to the well-known fire triangle that displays the three key points for a fire to occur, the criteria for a dust explosion can, extended with two additional factors, be shown in a pentagon as displayed in figure 1. [3]

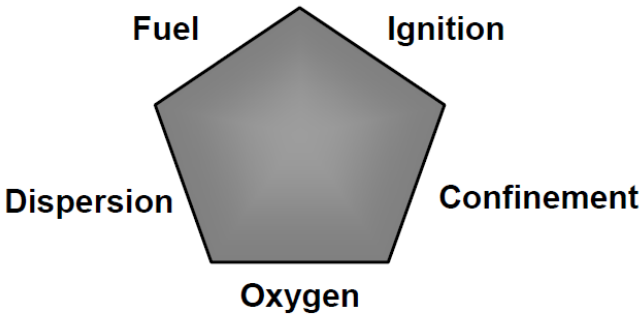

Figure 1: Dust explosion pentagon [2]

Due to the numerous cause variables that decide on the development of dust explosions, the resulting threat is in most cases difficult to assess and considerably differs from case to case. Hence, it is crucial to quantify the flammability and explosion properties as well as possible. For this reason numerous safety indices have been developed in that context. Those indices mostly represent quantities that are strongly dependent on the type of testing method that was used, this should be kept in mind when comparing values especially in case of different origins. For the case studies that were carried out within this thesis, only two safety indices were determined. The reason for this is the priorly described problem that comes up when comparing results that

were generated in different geometries or under different conditions. The first quantity that was determined for all kinds of additives of different grain sizes was the Minimum Ignition Energy. The second value to be calculated was the flame propagation speed. Other very important indices which are not further treated within this work are the Maximum Explosion Overpressure, the Maximum Rate of Pressure Rise, upper and lower explosion limits and ignition temperature. [3]

2.1.1 Minimum Ignition Energy

As indicated by its name, the Minimum Ignition Energy constitutes the minimum energy necessary for the ignition of a flammable dust cloud, commonly specified for electric sparks. It can be understood as a measure for the ease with which an explosion can be induced. A common apparatus to determine this value is the modified Hartmann tube, a vertical glass pipe in which dust is injected and dispersed by pressurized air. The predefined amount of energy is provided by an electric spark occurring between two electrodes in the pipe. Figure 2 shows the basic experimental setup. [5]

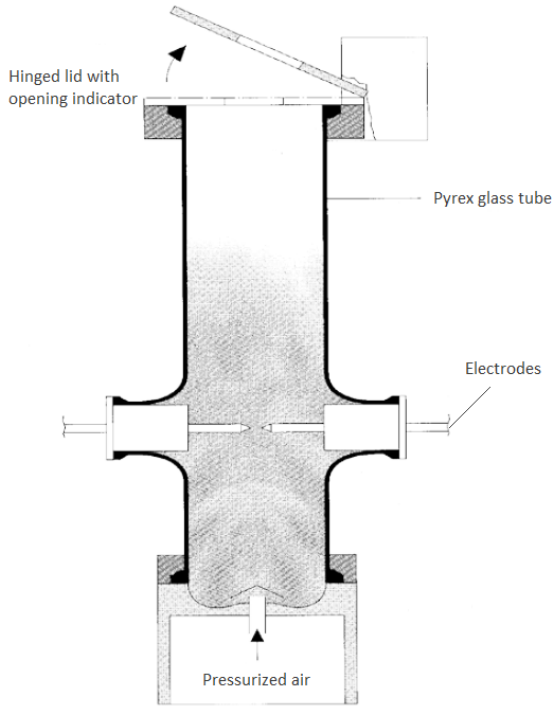

Figure 2: Modified Hartmann apparatus [4]

Although settings are held stable for several runs, altering conditions such as inhomogeneous dust concentrations are likely to occur. Reaching the range close to the MIE of a specific sample, both ignition and no ignition can be observed. More precisely, the boundary between the two possible outcomes is rather blurry and a specific value sparsely informative. Therefore the ignition energy is calculated as a function of a higher and a lower energy level where in the

first case ignition takes place and in the second not, considering the number of successful ignitions in relation to the total number of attempts. Keeping this in mind, it becomes clear that the ignition energy can only be a statistical quantity and no physical constant and should therefore be treated with caution. Within this thesis only one value for the ignition energy of a specific system was determined. By definition this is not the same as the standardized Minimum Ignition Energy which requires several runs of experimental tests to be calculated. In order not to provoke confusions the necessary energy input for ignition determined via simulations is simply described as the ignition energy.

2.1.2 Flame Propagation Speed

Phenomena of flame propagation in combustible aerosols play an important role for a better understanding of dust explosions. Simultaneously, they constitute a very complex field of research due to the heterogeneous nature of the system. This mentioned complexity stems from the interaction between different coexisting phases, more precisely from the transport of mass, momentum and energy between them. [6]

In the light of the above, the flame propagation speed is an important variable to determine. Methods aiming to quantify it basically track the local proceeding of the flame front. Experimentally this can be done using high speed cameras. Chen et al. for example conducted a study on flame propagation in solid 1-Octadecanol dust determining its velocity by means of a CCD video camera [8]. In [7], Proust describes similar experimental tests with focus on starch containing flammable mixtures. A very important factor that has to be considered when comparing results of the simulation with experimental data is the dependency of propagation velocities on the testing geometry. Only geometries with similar measurements can be used for this purpose.

2.2 Thermochemistry of Dust Explosions

Assuming the adiabatic combustion of a fuel in the oxygen present in air, the internal energy of the system remains constant in accordance with the first law of thermodynamics. The surplus of chemical energy deriving from the different energy levels of educts and products is transformed to heat. The temperature in the system increases, leading to elevated reaction speed which causes even faster release of heat. As no dissipation occurs the adiabatic temperature constitutes coincidently the maximum theoretical temperature.[11]

Under real conditions the system is always exposed to heat loss due to radiation, cooling walls, dissociation etc. [11]. Setting up an energy balance which compares the heat flux due to combustion with the removal of heat, one can learn a lot about the reaction behaviour from a chronological point of view. Figure 3 shows a heat balance for a reaction that is capable of a thermal run-away. This is a state in which the exothermic reaction gets out of control, likely ending up in an explosion. It can be seen that below the unstable stationary point USP, more

heat is removed than generated, always returning the system to the stable point displayed in the lower left corner of the graphic. In the case that enough heat is supplied for exceeding the USP, a dangerous cycle of increasing reaction rates causing higher temperatures and vice versa starts, leading to a very fast and disruptive reaction.

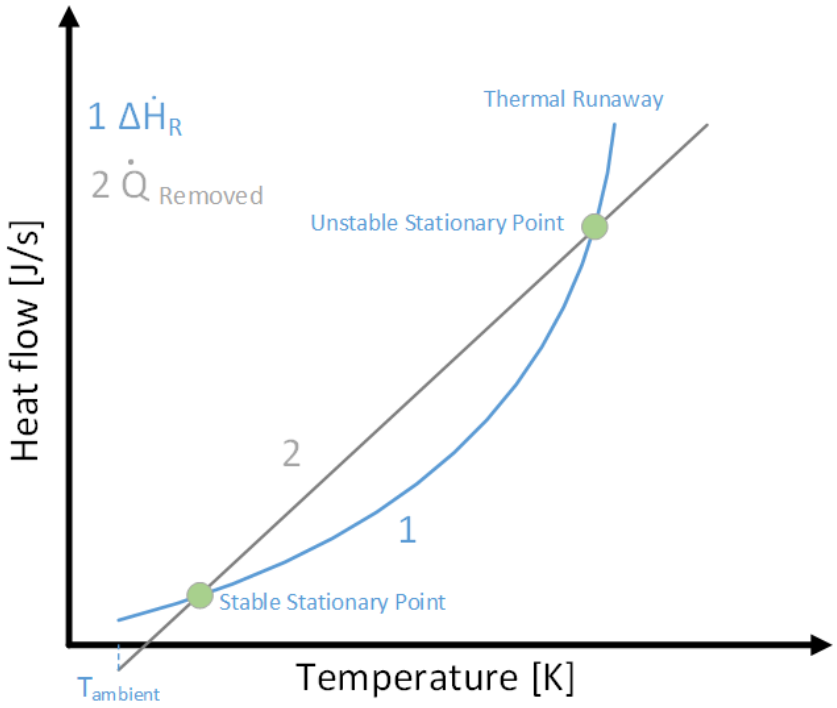

Figure 3: Thermal energy balance for an exothermic reaction as a function of temperature [12]

2.3 Fundamentals of Flame Extinction/ Suppression

Similar obligatory requirements as applied to the ignition of fuel, which has already been discussed in 2.3, exist for the self-sustainment of a flame. Firstly, violent combustion reactions can only occur between an upper and a lower concentration limit. Secondly, fuel and oxygen have to be well mixed in order to react in relevant quantities. Thirdly, complete reaction of educts to end products can only succeed when all intermediate steps take place and lastly enough heat has to be retained in the system to deliver the activation energy for the proceeding combustion.

Considering this from the perspective of flame extinction, one can conclude that prohibiting one of these conditions must lead to the desired success. Indeed, research done on this topic in the last few decades revealed several mechanisms that proved to be relevant in flame extinction. They are listed below, whereby the two latter issues are not going to be further investigated within this thesis, but were appended for the sake of completeness:

- Extraction of heat [9]
- Oxygen displacement [9]
- Dilution [9]
- Blocking of radiant heat [9]
- Interruption of chain reactions - trapping free radicals [10]

To what extent each of these mechanisms contributes to the extinction/suppression of flames varies significantly from case to case. Phenomena of mutual enhancement are just as possible as mutual weakening of coexisting extinction effects. [10] The main focus of this work was placed on the extraction of heat from the combustion zone, more extensive information on this topic can be found in 2.3.1.

2.3.1 Extraction of Heat

Thermal mechanisms interfere with the supply of energy necessary for the preservation of a flame. Recalling the balance of figure 3 the temperature in a system is decreasing when the heat loss exceeds the release of reaction energy per unit time. Below a certain level the flame cannot persist by its self-generated heat and is extinguished [11].

As combustions of gaseous hydrocarbons are strongly exothermic, their extinction requires high-performing heat sinks. Another important role plays the factor time because of very high combustion rates they are confronted with. Maybe the most important property of extinguishing powders is their competitiveness in terms of their thermal resistance. Briefly summarised, powders acting successfully as extinguishing medium in dust explosions should respond quickly to an input of heat and be capable of absorbing great amounts of energy.

2.4 Fundamentals of CFD Modelling

2.4.1 OpenFOAM ®

To perform simulations of dust explosions in the presence of different dispersed inert powders the open-source CFD software OpenFOAM® (Field Operation and Manipulation) was used. It is based on C++ code and a very mighty tool for solving complex problems in the field of fluid dynamics. Unlike commercially available products, OpenFOAM® has no user interface and is started via a command line. Very characterisitic for the software is its extensive file structure. All the information OpenFOAM® needs for running is provided in text files that are closely interlaced between each other. A specific case consists of three main folders, one contains all initial conditions, one the constant properties, settings and mesh data while the last one specifies all information relevant for the numerical solution. In the so-called solver the conservation equations

for quantities such as density, velocity and energy as well as submodels are solved for each cell.[19]

The coalChemistryFoam Solver

Simulations for this thesis were all run with an adaptation of the solver OpenFOAM® provides for the calculation of coal combustions with the possibility to introduce inert particles into the system. The basic $coalChemistryFoam$ is able to calculate transient compressible turbulent flow with combustion reactions. Pollhammer [1] describes what amendments have to be made in order to model lycopodium instead of coal particles and to introduce a time-dependent heat source similar to an electric spark.

2.4.2 Euler-Lagrangian Approach

The cases being covered in this thesis all show a particle-laden flow regime. For this purpose an Euler-Lagrangian approach is well-suited. The gaseous phase is regarded as a continuum in whose framework the dispersed solid particles are tracked. [13]

Depending on the transport directions of conserved quantities, such as mass, momentum and energy, one distinguishes between one- and two-way coupling. One-way coupling implies that the gas phase influences the solid particles but not vice versa. Two-way coupling, which is used for the cases within this thesis, considers mutual affecting between phases. The interaction of particles and fluid considers aerodynamic drag which occurs at the boundary face between them, the transfer of momentum and turbulent kinetic energy from the particles and the transfer of turbulence from gas to the solid phase. [14] Additionally, transfer of heat and mass for example from liquid-laden particles in the form of vapour can also be modelled. For all terms that describe the transition of a quantity between the phases the conservation equation on the fluid side contains a source term. More information on how a conservation equation is structured can be found in section 3.

2.4.3 Particle Clustering

The solution of the Lagrangian phase requires high computing performance as properties need to be determined for each single particle. In order to reach specific concentrations in bigger geometries particle numbers up to several millions can occur. For this case the concept of $Clustering$ was developed. Behind this concept stands the simplification that the properties of one particle are calculated and transferred to a user specified number of particles that are aggregated in a group defined as one parcel. The disadvantage of this method is that bulk behaviour cannot be displayed correctly as particles contained in one parcel don't "feel" each others presence. Therefore, the number of particles in a parcel should be chosen with caution. Generally it is assumed that by keeping the volume fraction of the particles in a parcel below one volume percent of the enclosing cell the probability of collisions or other interactions are negligible. As a thumb rule for this thesis the parcel number was chosen according to the cell number in order to ensure that not more than one or two parcels are located in one cell.

2.4.4 OpenFOAM's particle classes

OpenFOAM® provides a number of particle classes that differ from each other by means of their features. Starting from very low functionality, basically the uncoupled transport in an Eulerian phase, each further class gains more capacities (see table 1). Thereby, subsequent classes assume the features of the previous ones, this central concept of C++ programming is called inheritance.

Table 1: Features of different particle classes in OpenFOAM 2.4 (optional one/two way coupling)

parcle class	features
coalParcel	surface reaction features of MultiphaseReactingParcel features of ReactingParcel features of ThermoParcel features of KinematicParcel
MultiphaseReactingParcel	film modelling multiphase composition devolatilisation features of Reacting Parcel features of ThermoParcel features of KinematicParcel
ReactingParcel	reaction phase change features of ThermoParcel features of KinematicParcel
ThermoParcel	heat transfer features of KinematicParcel
CollidingParcel	particle- particle collisions
KinematicParcel	drag turbulent dispersion wall interactions

2.4.5 Conservation Equations

In CFD modelling conservation equations for quantities that can neither be created nor destroyed are used to calculate specific variables of interest. For example, the temperature in a cell can be calculated on the basis of an energy balance set up inside its boundary faces. The structure of conservation equations is independent from the type of quantity that is observed. The temporal variation of a variable in a control volume is result of its transport to and from its boundaries, either by convection or diffusion and the change that stems from the presence of source and sink terms within the observed volume. A simple form of an energy conservation equation is presented in Figure 4. Radiation is treated as a source term but stated separately

due to its importance as a heat transport mechanism. In fluid dynamics a system is described via three basic conservation equations namely one each for momentum, mass and energy.

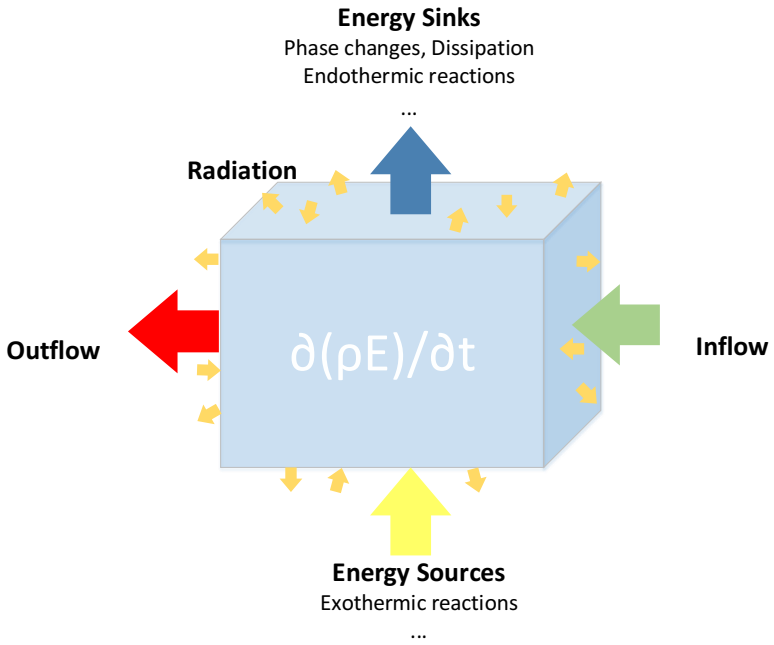

Figure 4: Contributing terms in a basic energy conservation equation

2.5 Turbulence

Concerning its mixing behaviour the heterogeneous lycopodium/air system ranges between the two marginal cases, ideally stirred reactor and plug flow. For the first-mentioned type no diffusion-limitation on molecular level occurs and the reaction is only depending on kinetics. The second type describes a completely diffusion-limited reaction where no mixing can be observed. The partially stirred reactor which is used for modelling the combustion of $C_{16}H_{34}$-vapour in air takes into account both factors. Considering the fact that the observed system is not premixed, diffusion plays an important role for the proceeding reaction.

2.5.1 Molecular vs. Turbulent Diffusion [16]

If in the context of chemical reactions the mixing behaviour in a system is considered, it always refers to micro-mixing which takes place on a molecular level. First and foremost the frequency of contact between the particles of participating gases is determining the reaction rates. Two diffusive processes can be accounted for influencing the likelihood of collisions, both occurring on different length scales. In order to reach certain reaction rates the interaction of the two of them is required. Molecular diffusion is a rather slow process and due to this its

influence is limited to very small scales. It is crucial for reaching a homogeneous distribution of molecules that enhances the contact but in fast reactions shows insufficient mixing capabilities. According to the equation of Sutherland its constant of proportionality is dependent on the material specific value of viscosity and the state variables temperature and pressure. In contrast, turbulent diffusion is very effective when it comes to mixing down to scales of the size of the smallest occurring eddies. Within the breakup process of bigger eddies into smaller eddies the segregation is downsized. By limiting the distances molecular diffusion has to overcome in order to create well mixed regions turbulent diffusion enhances reaction rates. Figure 5 displays how both processes influence micro-mixing. In (a) the impact of turbulent diffusion is shown while (b) depicts molecular diffusion. In (c) the superimposed processes are shown together.

2.5.2 Turbulence Modelling [15]

Accurate modelling of turbulence in Computational Fluid Dynamics is a very important aspect that strongly affects the quality of the gathered data. From figure 6 one can already derive main features of a turbulent flow. Firstly, it shows random and chaotic behaviour and develops unpredictably in all directions. Secondly, the vortex size reaches from geometry dimension to the Kolmogorov length, which is a function of viscosity and dissipation energy ϵ and normally reaches a few millimetres or less. The largest eddies withdraw kinetic energy from the main flow and pass it on to smaller ones that do the same with even smaller ones. This proceeding is continued until the energy has reached the smallest eddies that dissipate it due to viscous forces into internal energy. The whole process is called cascade process and the dissipated energy is expressed by the quantity ϵ.

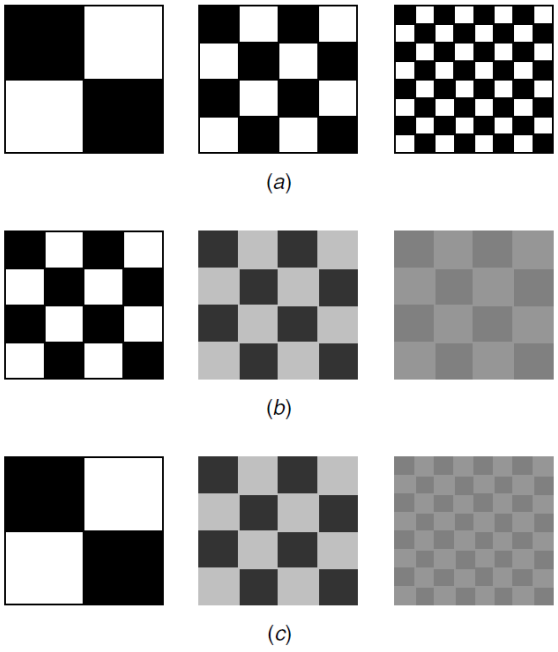

Figure 5: Turbulent vs. molecular diffusion influence on micro-mixing [16]

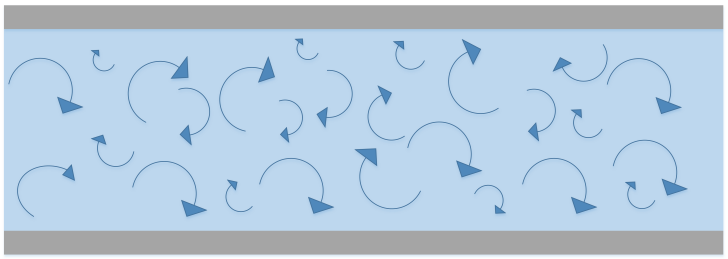

Figure 6: Random formation of vortexes in turbulent flow

The problem that occurs when modelling turbulent flow is that due to the random vortex appearance no stationary conditions develop and quantities are at any point functions of space and time. The complete resolution of the Navier-Stokes equation for momentum conservation in a turbulent flow is called Direct Numerical Simulation DNS and takes for very simple problems and current computer performance several decades. Therefore it is necessary to implement a turbulence model that simplifies the Navier-Stokes equation and accelerates calculation. Most of the turbulence models are based on the time averaged version of the equation that splits up terms into a fluctuating and an average part. This step creates a closing problem by adding a supplementary term to the total shear stress that is called Reynolds stress. Turbulence models offer direct values or correlations for this term in order to make the NS-equation solvable. Not all turbulence models fit to all physical problems and the choice should be made with caution.

For the simulations done within this thesis the two-equation model $k - epsilon$ was chosen. It uses an approach that expresses the Reynolds stress by an introduced turbulent viscosity μ_t that is multiplied by the velocity gradients. In order to get this viscosity value, the model provides two conservation equations one for turbulent kinetic energy k and one for the dissipated energy ϵ from which the value can be deduced. The two conservation equations are structured similar to the ones discussed in 2.4.5. As source terms both have a production as well as a dissipation term. In the the k-equation ϵ is implemented as a sink term. Again both equations cannot be solved on the spot and some terms have to be simplified and expressed by means of empirical correlations. For more detailed explanations and derivations the reader is referred to numerous books, lecture notes and articles dealing with this extensive topic for example Davidson [15].

2.5.3 Particle Interaction with Turbulence [17]

Particles inserted into a continuous flow influence its intensity of turbulence by either adding or removing turbulent kinetic energy. Brennen [17] states that whether they add or remove energy strongly depends on the particle size. Large particles show relative motions in a flow due to their comparatively high inertia which creates waves that lead to additional turbulence in the system. Very small particles can follow the flow very well and while doing so, they absorb turbulent kinetic energy. Consequentially, one can conclude that the lower relative motions between Eulerian and Langrangian phase are, the more kinetic energy can be transferred between them.

2.5.4 Modelling of Particle Motions in Turbulent Flow [18]

By solving the time averaged Navier-Stokes equation using a turbulence model for the closure problem, the instantaneous velocity components for the flow field vanish. To model a proper particle distribution in the turbulent flow its contribution has to be estimated. The random and chaotic development of eddies suggests the usage of a stochastic method for this purpose. In the so-called discrete random walk model the fluctuating part is set on basis of a Gaussian distribution function. The standard deviation from the time-averaged velocity component is expressed as a function of of turbulent kinetic energy k that is by definition a function of the fluctuating velocity. For the validity of the model isotropic development of eddies has to be assumed. The variance from the mean velocity is the square of the instantaneous component. Equation 2–1 expresses the standard deviation by means of the turbulent kinetic energy k.

$$\sigma = \sqrt[2]{2 * k/3} \tag{2–1}$$

in order to consider the chaotic nature the instantaneous velocity component, it is calculated as a product of a random normally distributed value and the standard variance σ.

3 Quantitative Determination of Heat Sinks

In order to examine the ability of non-flammable powders to act as a suppressant/ extinguishing medium in dust explosions it was assumed being beneficial to know, to what extent they can absorb heat from the proceeding combustion. Solely determining the energy transferred to the inert particles raises the problem, that the relation to other source terms is missing. Therefore the aim was to capture all sources that contribute to the energy equation in order to get a complete energy balance for the whole system.

As already mentioned in 2.4.2 the $coalChemistryFoam$ solver calculates the energy conservation equation for each cell of the gas phase considering the Lagranian phase(s) as source terms on the right side. By default only temperature and heat capacity are written out for each time step. Consequentially, the solver had to be adapted in a way that enables the recording of source terms as scalar fields and hence assigns a value of energy dimension to each cell.

3.1 Solver Set-Up

In the solver directory several files can be found OpenFoam® accesses in order to compute specific CFD-problems. Depending on the scope or more precisely on the capabilities a model should have, the number can vary. As $coalChemistryFoam$ deals with models that include multiple phases, turbulence and combustion, its directory looks like shown in figure 7. Files that are marked with $*Eqn.H$ contain conservation equations for mass (rho), energy (E), momentum(U) and mass fraction (Y) for the components of the gas phase as well as the continuity equation expressed by pressure (p). In the $createFields.H$- file type of field and dimension is specified for each variable of the gas phase. In the $createClouds.H$- file the clouds are specified by assigning them name and type of cloud class.

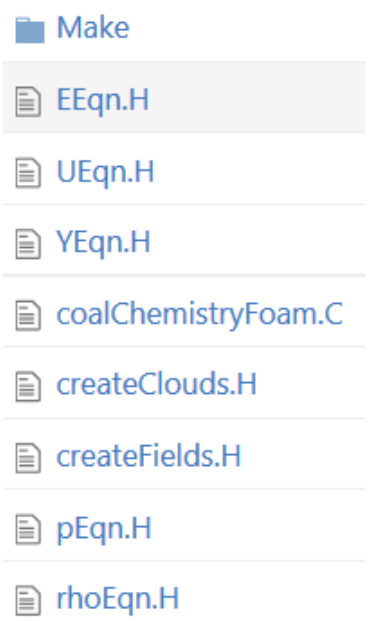

Figure 7: Files in the folder directory of the coalChemistryFoam solver in the version OpenFOAM 2.4

3.2 Structure of the Energy Conservation Equation in OpenFOAM® [20]

OpenFOAM® is solving a conservation equation for the total energy considering mechanical and thermodynamic contribution. Being aware of 2.4.5 the basic set up of the equation can be mathematically expressed by equation 3–2.

$$\rho * \frac{de}{dt} + \rho * \frac{dK}{dt} = -\nabla * q + \nabla * (\sigma * U) + \sum \rho * r + \rho * g * U \tag{3–2}$$

The two terms on the left hand side of the equation are the total derivatives of thermodynamic (e) and mechanical (K) energy. For quantities that are a function of time and space the term can be split up in local derivatives. One thereby covers the temporal change at a specific position (x, y, z) and the other one considers the transport of a quantity with velocity U. The first term on the right hand side is a diffusive transport term for the thermal energy and $\rho * r$ its source term. The second and third term on the right side of equation 3–3 are flux and sources for mechanical energy similar to the thermal ones mentioned before. After several transformations and replacement of internal energy e by the enthalpy h, the equation becomes 3–3. The detailed

derivation of the equation from the beginning to the final state can be found in [20].

$$\frac{\partial(\rho * h)}{\partial t} + \nabla(\rho * U * h) + \frac{\partial(\rho * K)}{\partial t}\nabla * (\rho * U * K) - \frac{\partial p}{\partial t} = \\ -\nabla * q + \nabla * (\tau * u) + \rho * g * U + \sum \rho * r \tag{3–3}$$

3.3 Adaptation of the coalChemistryFoam Solver

In figure 8 the C++ based code for the energy conservation equation is shown. In order to be able to write out additional fields for each time step, it is necessary to specify them in the createFields.H file with the appropriate dimensions.

As can be seen in figure 8 OpenFOAM® differentiates between terms specified as fvm and fvc. Through this preliminary declaration the numerical solution scheme is set. fvm stands for implicit numerical solutions, which means that a variable is dependend on other variables of the same time level. This approach generates a system of equations with unknowns on both sides of the equal sign that can only be solved via interpolation. Terms that are declared as fvm give back matrices and not fields. By contrast, explicit solutions are calculated on the basis of values from previous time steps that are already known. Terms of that type give back fields in which a value is assigned to each cell.

```
fvScalarMatrix EEqn
(
    fvm::ddt(rho, he) + mvConvection->fvmDiv(phi, he)
  + fvc::ddt(rho, K) + fvc::div(phi, K)
  + (
        he.name() == "e"
      ? fvc::div
        (
            fvc::absolute(phi/fvc::interpolate(rho), U),
            p,
            "div(phiv,p)"
        )
      : -dpdt
    )
  - fvm::laplacian(turbulence->alphaEff(), he)
 ==
    rho*(U&g)
  + combustion->Sh()
  + coalParcels.Sh(he)
  + limestoneParcels.Sh(he)
  + radiation->Sh(thermo)
  + fvOptions(rho, he)
);
```

Figure 8: Energy equation of the coalChemistryFoam Solver in OpenFoam 2.4.0

The source term of combustion gives back a Volume Scalar Field by default and can be easily

saved under a new variable. The other source terms listed in figure 8 turned out to be implicit and needed to be transferred from matrix to field format. One possibility for doing this was to implement a new quantity instead of energy. By equating the rate of change for this property with the considered source term one receives a scalar field of an energy parameter. 3–4 shows the resulting equation representative for all implicitly solved source terms.

$$\frac{\partial(\rho * E_{new})}{\partial t} = S_Q \tag{3–4}$$

The obtained quantity is related to the amount of energy that is transferred either from or to the gas phase of each cell. The dimensions that come along with energy source terms are shown in table 2. The column on the right describes the post-processing steps necessary to get values in Joule. Further informations on this topic follow in 3.5.

Table 2: Dimensional analysis of energy source terms

Energy source terms	Dimensions	Post-processing
combustion	$kgm^{-1}s^{-3}$	Integration over Volume V Integration over time t
coalParcels	Jkg^{-1}	Multiplying by ρ Integration over Volume V
limestoneParcels	Jkg^{-1}	Multiplying by ρ Integration over Volume V
radiation	Jkg^{-1}	Multiplying by ρ Integration over Volume V

3.4 Case Set-Up for the Test Geometry

In order to validate the functionality of the adapted solver a one dimensional test geometry was observed. In the bar that can be seen in figure 9 were Lagrangian particles of around $120\ g/m^3$ of the geometry. They were randomly arranged along the y-axis but with constant and equal distance to x- and z-axis. The boundary conditions for the simple testing geometry were selected in a manner that enabled creating an adiabatic system. This way, it was ensured that no energy could leave the observed room via outer surfaces. As shown in figure 9 the bar stretches along the y-axis and is lengthwise partitioned into 100 cells. In x- and z- direction the geometry has only a thickness of one cell width. Particularly for this case OpenFOAM® provides a boundary condition defined as empty that treats the geometry expansion in these directions as non-existent. In the 1-D geometry only two faces show boundary conditions other than empty. A no-slip condition was assigned to both of them in terms of velocity and a Neumann-boundary

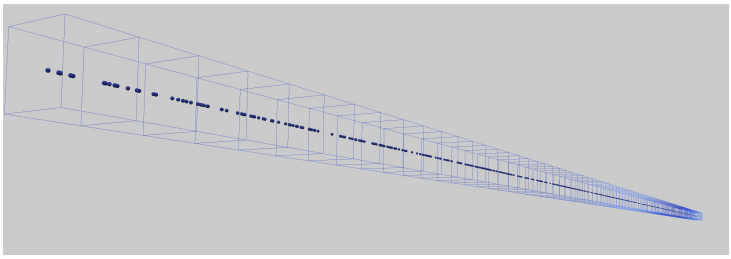

Figure 9: one-dimensional geometry for testing the functionality of the modified coalChemistryFoam solver

condition($\nabla P = 0$) was chosen for pressure as well as temperature. In OpenFOAM® this type of boundary condition is implemented as $zeroGradient$. The uniform temperature of the gas phase was set to $350K$ while for the solid particles $300K$ were chosen. Their only thermal contribution to the energy conservation equation originated from heat capacity. Due to the simple set-up of the case with only one particle class and neither phase change nor chemical reactions the source terms for the second particle class (limestoneParcels), combustion and electric spark($setQ$) were zero.

In order to run the case with the newly generated solver from 3.3 the solution settings in the system folder of the case needed to be supplemented. For the newly introduced energy variables, information had to be specified on how they should be solved. This is done by adding a new block of entries for each of them in the $fvSolution$ file. Once this was done, the case could be started.

3.5 Post-processing in Paraview® and Matlab®

OpenFOAM® writes out data in an interval that can be set by the user in the control dictionary of a case. The informations are recorded in text files, one for each variable and again structured in a directory of folders with the one on top being named by the current time step. As OpenFoam® has no graphical interface, for visualisation and processing of data it comes with the open-source software Paraview® that can be started directly from the command line by default. The software provides numerous post-processing features, among them the possibility of executing arithmetic operations with field variables and integration over volume.

Methodology in Post-Processing

Compendiously, within this thesis the focus was placed on identifying heat sources and heat sinks in simulated dust explosions. The terms expressing the contribution of particles and radiation in the energy equations occur in the dimension of J/kg whereas for reasons of comparability Joule are required. The values are given as fields, one assigned to each cell

although the whole system should be considered. Carrying out a dimensional analysis makes clear, that the terms need to be multiplied by the density of the gas phase and then integrated over the volume. Described in basic arithmetic operations, the field values are initially multiplied by the cell volume and subsequently summed up over the whole geometry. Thereby, one single source term for each time step is generated. Other variables such as temperature and velocity that are not related to a specific volume must be divided through the total volume after integration in order to get values in common form. This procedure corresponds to the determination of a mean value for the whole system at each time step. The source term for combustion has the dimension $Jm^{-3}s^{-1}$ and needs to be integrated over volume as well. Additionally an integration over time is necessary in order to get a value in Joule. The methodology for each term can also be found in the right column of table 2. Operations tracking the over-all temporal progression of a variable are better done with data processing software, in this case Matlab®. From Paraview® data sets can be written out time step by time step in a sequence of numbered CSV files.

Depending on the temporal resolution of a case a complete data set can consist of several hundred files and the manual input is simply not efficient. Therefore a Matlab® program was written that is able to open one file after the other transferring the included values into an array. At the end, each column contains the values of one quantity and each line the values of one time step.

3.6 Analysis of the Energy Transfer Between Particles and Gas Phase

The aim of running the test case was to check whether the energy loss from the gas phase and the heat absorption by solid particles correspond to the emitted source term values. The amount of energy that is stored in the gas phase due to the material's heat capacity can be calculated according to equation 3–5.

$$E_{therm} = c_p * \rho * V * T \tag{3–5}$$

Analogous procedure can be applied to the solid particles. In order to determine the change of heat within the phases, the difference between their energy states at the first and last time step are considered as described in equation 3–6.

$$\triangle E_{therm} = c_p * \rho * V * (T_E - T_I) \tag{3–6}$$

For the gas phase calculations on the basis of equation 3–5 can be carried out in Paraview®. The values necessary for calculations with regard to the solid phase were taken directly from OpenFoam's data folders. The files were transferred to $*.txt$ format and read in Matlab®.

After finishing the post-processing, three values are available for evaluating the functionality of the solver. One gives back the energy decrease in the gas phase and one the energy increase

in the particles both on the basis of OpenFOAM®'s temperature, heat capacity, density and volume. The last one constitutes the value that is calculated using the field data of the particle source term in the energy conservation equation. Putting them in relation captures the deviations between them. Table 3 contains the results of the study.

Table 3: Relative deviations [-] between amounts of transferred energy in an adiabatic system calculated by using three different approaches

c/l	thermal energy decrease in the gas phase	thermal energy increase in the particles	particle source term
$\triangle E_{Gas}$	-	1.1578	1.1645
$\triangle E_P$	0.8637	-	0.9943

Very good correspondence can be found between E_P and E_{Source} which is an indication for the proper recording of source terms. Between the energy decrease in the gas phase and the corresponding increase of heat for the solid particles a deviation of 15% can be observed. Principally, it is sensible that both values do not equal each other completely as other terms such as radiation and contribution of terms covering mechanical energy have an uncontrollable impact on the energy distribution in the system. The quantity in which both values deviate from each other is rather surprising. Especially when considering that the case involves a closed adiabatic system with no initial flow velocity and low temperatures. In advance, one would ascribe to previously mentioned coexisting terms that they play only a subordinate rule. However, it could be shown that the newly introduced field variables display the energy contribution in the system very well.

4 Equipping the coalChemistryFoam Solver's Basic Inert Particles with New Physical Properties

4.1 Initial Case Set-Up

By default the $coalChemistryFoam$ solver contains a second parcel cloud of type $Thermo$ that can be used for investigating extinguishing effects of solid inert particles. Files and folder structure of the model aiming to determine the Minimal Ignition Energy are based on the corresponding tutorial case $SimplifiedSiwek$ in which the additional cloud is also included. For running the first cases only the particle properties had to be modified as required. Several materials were tested within the associated experiments that were carried out at the Chair of Thermal Processing Technology among them zeolite, a cristalline mineral. For solids OpenFOAM's database knows only three different materials namely ash, carbon and limestone. Fortunately it gives its users the option to switch off the reading of properties from the database. Instead one can implement own values directly in the $thermophysicalProperties$- file in the constant folder which was done using zeolite properties gathered from the vendour's product data sheet. As the simulations were aimed to reveal fundamental behaviour rather than specific data any realistic values could have been used. More information about the basic case set-up for the determination of ignition energy can be found in [1].

4.2 Water-Laden Particles

The idea behind testing the impact of water-laden particles on the flame propagation is that in two ways one would expect them to act against the proceeding of an explosion. Firstly evaporating water should be capable of acting as a heat sink and secondly the release of vapour

into the gas phase should lead to dilution and oxygen displacement. In order to model the above specified behaviour inert particles have to show the following additional abilities:

- Multiphase composition
- Evaporation

When recalling table 1 it becomes clear that for this purpose the initial $ThermoCloud$ needs to be replaced by a $MultiphaseReactingCloud$. The easiest approach is to introduce a second $coalCloud$ as this one is already properly implemented in the solver. The name $coalCloud$ is a bit confusing as one would automatically relate it to combustible particles but in fact the particle class is very useful as it combines the capabilities of multiphase composition, evaporation and surface reactions in one particle

4.2.1 Implementation of a Second coalCloud into the Case

Initially the new water-laden particles have to be specified as a "coalCloud". This is done in the $createClouds.H$ file. Originally only energy (E) and momentum (U) conservation equation contain a source term for the inert additives. Due to the evaporation of water from the designated "limestoneCloud", source terms are also transferred from the particles to the continuity equation (p) and the equations for mass fraction Y and density ρ. For this reason each of them had to be supplemented with the additional source term.

Besides the modifications in the solver, the particle properties in the case directory have to be adapted. The original properties contained a data range that was sufficient for describing a basic ThermoCloud but not for a "MultiphaseReactingCloud" (table 4). Therefore the existing file for coal parcels was copied and modified according to the requirements. The specifications for the $coalCloud$ in column 3 of table 4 can be adapted without changes. The terms defining devolatilisation and surface reaction can be set to none, but in the absence of a devolatilizing gas or carbon they do not give a contribution anyway. Many of the shown specifications require additional information in the form of coefficients. For water-laden particles their entries are shown in figure 10.

Table 4: Comparison of information contained in *properties-files for $Thermo$- and $coalCloud$ in OpenFOAM 2.4.0

Model	Specifications for a $ThermoCloud$	Specifications for a $MultiphaseReactingCloud$
Dispersion model	stochasticDispersionRAS	-//-
Patch interaction model	standardWallInteraction	-//-
Heat transfer model	Ranz-Marshall	-//-
Composition model	not available	singleMixtureFraction
Phase change model	not available	liquidEvaporation
Devolatilisation model	not available	constantRateDevolatilisation
Stochastic collision model	none	none
Surface reaction model	not available	COxidationKinetic-DiffusionLimitedRate
Surface film model	none	none
Radiation	on	on

4.2.2 Testing of the new Case Set-Up in the Simple Bar Geometry

For testing purposes the one-dimensional bar geometry was used again. This time no lycopodium particles were inserted but instead the same number of water-laden particles. The old "limestoneCloud" property file was replaced by the new one from 4.2.1. In order to induce the particles to emit water vapour the temperature in the gas phase was set to a value above evaporation temperature. On the one hand, it was tried to keep temperatures as low as possible to have a slow evaporation that requires several time steps to be complete. On the other hand, the energy stored in the gas phase had to be sufficient for displaying all three phases, namely the heat-up processes prior and subsequent to the evaporation and the evaporation itself.

A plausibility check was then carried out for the testing system where the focus was placed on a physically correct behaviour of the evaporating particles. In the beginning the problem arose that particles exceeded the evaporation temperature already before vaporisation of water had completed. At that point many different reasons were worth considering but the most promising approach seemed to be the closer examination of the phase change model. For the evaporation OpenFoam knows two different options that are eligible in the cloud properties in constant folder of the case, namely $liquidEvaporation$ and $liquidEvaporationBoil$.

A problem of OpenFOAM® is that these models are very sparsely documented but their choice can have a huge impact on the simulation's accuracy. A small explanation can mostly be found in the associated header file which is located somewhere in OpenFOAM's folder directory. In order to find these files the web address `https://github.com/OpenFOAM` turned out to be very useful. On this page the complete folder directories for OpenFOAM 2.1-2.4 are stored and

using the provided search function for specific files helps a lot orienting oneself in the extensive folder system. The $liquidEvaporationBoil.H$ file refers to a paper on which the model is based. In principle it considers the occurence of flash boiling that takes place when superheated liquids enter a low pressure region and vaporise very quickly [21]. This model is not of relevance for the observed water-laden particles so the simple liquidEvaporation is the right choice in this case. Furthermore a coefficient has to be specified in the particle properties file controlling how the enthalpy transfer in connection with the vaporisation is implemented. The right choice in this case constitutes the method of $enthalpyDifference$ (figure 10).

```
liquidEvaporationCoeffs
{
    enthalpyTransfer enthalpyDifference;

    activeLiquids
    (
        H2O
    );
}
```

Figure 10: Additional settings that need to be specified for an evaporation model

As reviewing the phase change model did not reveal the problem of non-physical behaviour, the original tutorial case in OpenFOAM 2.4 was taken and modified in a way that its limestone particles were able to evaporate water. This time the particles showed the expected behaviour. In order to find the difference between both cases, the files in the constant folder of the test case were replaced one after the other by the ones from the tutorial. At the end the thermophysical properties in the constant folder turned out to be the disturbing ones. The reason could not be completely clarified as the included data was consistent but being of different versions of OpenFOAM®.

5 Adding the Ability of Melting

After successfully implementing evaporation for inert particles, the next and more challenging stage was to give them the completely new functionality of melting. The idea was to adapt an existing model for surface reactions in a way that it was capable of simulating a phase transition from solid to liquid.

5.1 Folder Structure

Figure 11 gives an overview on relevant file paths in the $lagrangian$-directory that had to be studied in order to find suitable positions for adapting the code. The files included in the $parcel$-directory can be described as the framework for solving Lagrangian particles. They constitute the guideline on which basis the solution progresses. Submodels, functions and other informations are called from there and results are handed back to them subsequently. One example would be the $surfaceReactingModel$ from figure 11. Each parcel class has its own folder that contains at least one header and one C-file with the same name. While in the header file declarations of classes, functions and variables are implemented the actual calculations are done in the C-file.

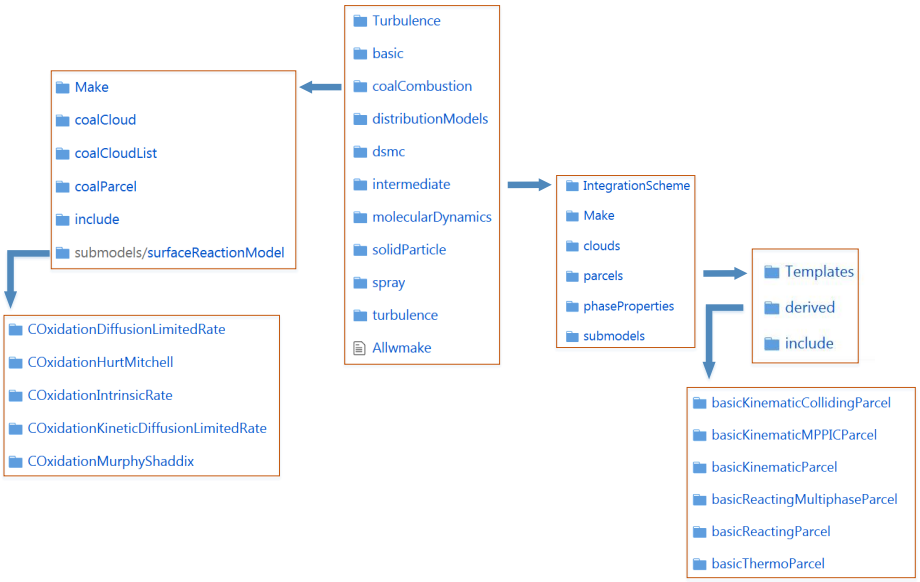

Figure 11: Folder structure in OpenFOAM's $lagrangian$ directory

5.2 Modification of a Surface Reaction Submodel

For simulating coal combustion on particle surfaces five submodels are implemented in OpenFOAM® by default. Their calling is controlled by the C-file of "MultiphaseReactingParcel"-class that checks their activity and hands over required information for calculating mass transition and energy contribution due to the reaction. In order to keep the development simple and prevent errors from occurring an already existing submodel was modified instead of creating a new one. OpenFOAM® has a very complex structure and it is sometimes difficult to find all the interdependencies between different files at once. By keeping the same name one ensures that all files that need to access the submodel can still find it. As there exist five of them it was no problem to transcribe one with the new melting functionality. The submodel "COxidationDiffusionLimitedRate" seemed to be best suited for the planned adaptations.

The physical process of melting is quite simple as its occurrence can be assigned to a fixed temperature - pressure combination. As long as solid material is present the total energy input is applied to the phase transition and no temperature increase can be observed. The core issue of the modification was therefore to provide information on how much energy was available for melting. By default the "MultiphaseReactingParcel.C" file hands over selected data to active surface reaction models. Considering 3.2 OF obviously creates variables that contain information on the transferred source terms between carrier phase and particles but at what temporal and

spatial point they are provided and what their value really describes was still to be investigated.

A first investigation of code revealed that a variable Sh describing an explicit enthalpy source term for particles and a variable $dhsTrans$ describing the sensible enthalpy transfer from the particles to the carrier phase exist. However, through the study it became also clear that these terms are calculated after executing the surface reaction submodel. Therefore they could not be used for this purpose. The second idea was to find an approach to express the available amount of energy by using default variables that can be seen in figure 12. The variables Sh and $dhsTrans$ are not handed over to the submodel as the table in figure 12 indicates. It includes variables for the complete function of surface reaction but was chosen for displaying also the definition of terms.

```
//- Calculate surface reactions
template<class TrackData>
void calcSurfaceReactions
(
    TrackData& td,
    const scalar dt,           // timestep
    const label cellI,         // owner cell
    const scalar d,            // diameter
    const scalar T,            // temperature
    const scalar mass,         // mass
    const label canCombust,     // 'can combust' flag
    const scalar N,            // flux of species emitted from particle
    const scalarField& YMix,   // mixture mass fractions
    const scalarField& YGas,   // gas-phase mass fractions
    const scalarField& YLiquid,// liquid-phase mass fractions
    const scalarField& YSolid, // solid-phase mass fractions
    scalarField& dMassSRGas,   // gas-phase mass transfer - local
    scalarField& dMassSRLiquid,// liquid-phase mass transfer - local
    scalarField& dMassSRSolid, // solid-phase mass transfer - local
    scalarField& dMassSRCarrier, // carrier phase mass transfer
    scalar& Sh,                // explicit particle enthalpy source
    scalar& dhsTrans           // sensible enthalpy transfer to carrier
) const;
```

Figure 12: Standard data handed over to surface reaction submodels from "MultiphaseReactionParcel.C"

The only available heat related term is the particle temperature T which is calculated before entering the surface reaction submodel. For this reason it is not possible to tell the particles within the associated file not to exceed a specific temperature level. The only possibility is to remove the surplus of energy that stems from exceeding the melting temperature and supply the phase transition with it. This means that as soon as a particle crosses a defined temperature limit, namely its melting point, heat is removed from it in an extent that corresponds to the resulting temperature difference. The content of energy that is saved as heat has already been described with equation 3–5. The energy that is transformed to heat of fusion can be calculated according to the following relation:

$$E_{trans} = c_p * m_{par} * (T_{Melt} - T_{Par}) \tag{5–7}$$

Particle mass m_{par} and temperature T are default variables of the submodel and can be used instantaneously while the heat capacity c_p is a function of temperature and not known in the related files just like the enthalpy of fusion for the melting material. As time steps for the executed cases are very small and temperature differences are therefore very low the value is assumed to be constant for the complete melting process. This simplifies the implementation a lot. Still both values are unknown but can be accessed from the particle cloud property file in the $constant$-folder of the case. Under the item of surface reaction coefficients the missing quantities can be set. The corresponding phase transition of mass can be calculated by:

$$m_{trans} = c_p * m_{par} * (T_{Melt} - T_{Par}) / \triangle H_{fus} \tag{5–8}$$

Basically one has to distinguish between three different events that happen to occur and therefore have to be covered in the code. Once the particle has reached the melting point the main process starts characterized by the presence of enough solid mass to melt exactly the amount of material given by the available surplus of energy. The second case is that more energy than mass is available and the particle completely fuses and increases its temperature due to the remaining heat. The third case is that no solid material is contained in a particle any more and besides the heat capacity of the liquid no additional energy can be removed from the gas phase. Figure 13 displays the principal structure of the implemented code into the $COxidationDiffusionLimitedRate$ submodel.

On basis of the energy value returned from the submodel, the $MultiphaseReactingParcel.C$ file provides all the information necessary for the calculation of the actual source term for each surface reaction. By default, a coefficient apportions the main part of the source term to the particle and the rest to the gas phase. In fact the gas phase supplies the heat for the melting process but through the transfer on the particles. Therefore this approach is undesirable for a melting process. The problem with modifying the main files of the Lagrangian particles is that changes are valid for all calculated clouds. It is always necessary to implement a specific condition that ensures adaptations are only applied to correspondent particles. In this case the sign of the value could be used to realise different handling.

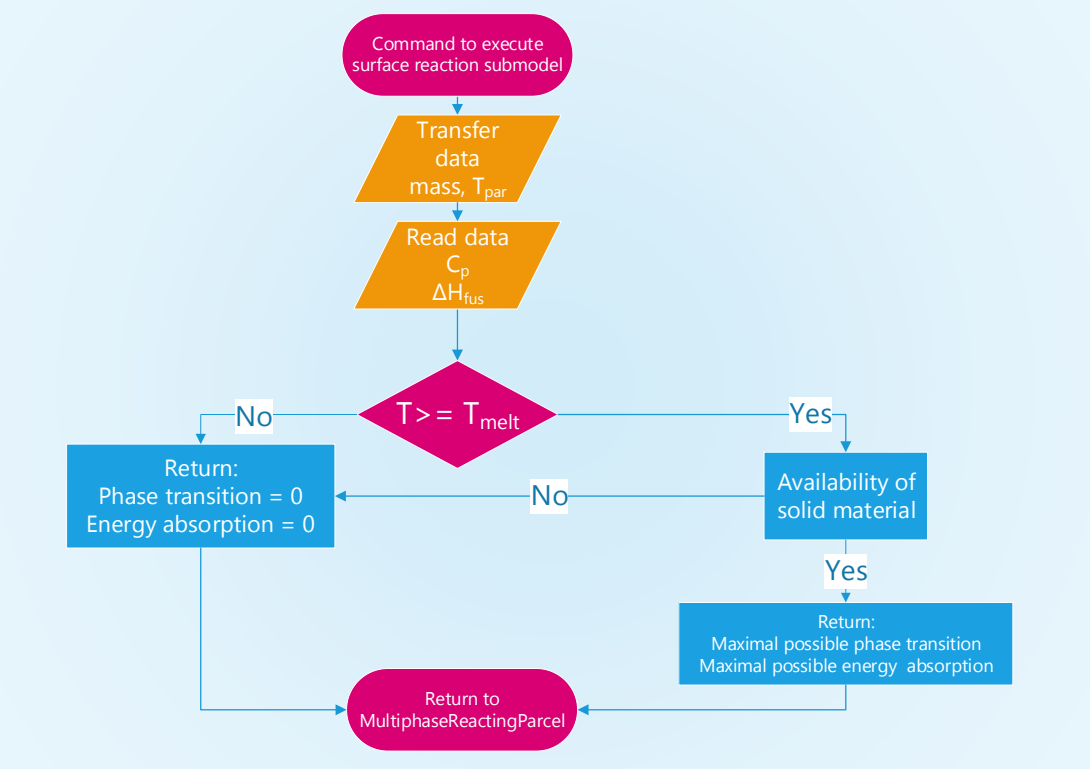

Figure 13: Graphical presentation of the newly introduced code in a surface reaction submodel

5.3 Testing the New Functionality in a Simple Geometry

After successfully compiling the modified folders, everything was again tested on a very simple geometry. For this purpose the solver had to be edited again. The evaporating particles interact with the gas phase through energy, momentum and mass exchange while the melting particles contribute source terms only to the conservation equations of the first two items. Moreover, a new material was added to the standard solid and liquid material database. The inserted properties were inspired by low-melting salts but cannot be associated with one specific material. The focus of the study was to investigate fundamental mechanisms and basic functionalities an applicable substance should have. This time there was no experience at all concerning the proper reproduction of the physical process, so in parallel a Matlab® code was written calculating a simplified version of the OpenFOAM® test case. It has to be mentioned that this proceeding did not aim to verify one or the other result but to get a better sense for plausible time ranges to complete a melting process. In order to check the phase transition behaviour tracking a single particle was enough. The heat up process of the particle was modelled on the

basis of an enthalpy (h) conservation equation (5–9).

$$\frac{\partial(\rho * h)}{\partial t} + \frac{\partial(\rho * u_j * h)}{\partial x_j} = -\frac{\partial \dot{q_j}}{\partial x_j} + S_Q \tag{5–9}$$

By default, OpenFoam® does not consider temperature gradients in Lagrangian particles and $\dot{q_j}$ can be expressed through Fourier's law given by:

$$\dot{q_j} = -\lambda * \frac{\partial T}{\partial x_j} \tag{5–10}$$

Consequentially heat conduction within the particle has to be neglected. For particles with low Biot-Numbers this simplification is permissible as only a small error is made due to it. Pollhammer [1] could show that for the observed particles this condition is met.

Moreover, the gas phase in the test case is initialised without flow and the only movement of its molecules is due to thermal effects. In order to keep them negligible the gas phase is designed many times bigger than the particle. This proceeding creates a homogeneous and nearly constant temperature field with very small gradients.

The differential expression for an enthalpy change in a system can be expressed as follows:

$$dh = du + d(p * V) \tag{5–11}$$

with

$$du = dq - pdV \tag{5–12}$$

Uniting equations 5–11 and 5–12 results in:

$$dh = dq + Vdp \tag{5–13}$$

If now dq is expressed through heat capacity and temperature and changes in pressure are neglected, one gets the simplified enthalpy conservation equation that is now a function of temperature:

$$\frac{\partial(\rho * c_P * T)}{\partial t} = S_Q \tag{5–14}$$

Yet the equation contains specific values. The integration over the particle volume gives a total value. Volume and density have to be considered as constant over time. This approximation was used in OpenFOAM® as well as in Matlab®. Both variables can be removed from the partial derivative and replaced by mass m. The source term S_Q on the right side of the equation 5–14 includes the heat transition from the gas phase to the particle that can be described by the

following mathematical term:

$$\dot{Q} = \alpha * A * (T_G - T) \tag{5–15}$$

As already mentioned, T_G can be assumed as constant due to the carrier phases's large size relative to the Lagrangian particle. Now all contributing terms have been specified. Equating 5–14 and 5–15, separating temperature T and time t and subsequently applying the substitution rule for the unknown variable T gives:

$$-ln(T_G - T) + C = \alpha * A * t \tag{5–16}$$

The terminal version of the equation after a few transformations and inserting the initial condition for expressing C can be seen in

$$T = T_G - (T_G - T_{P,0}) * e^{\frac{-\alpha * A * t}{m_P * c_p}} \tag{5–17}$$

For calculating the heat transfer coefficient α the Ranz-Marshall correlation was chosen. Once the particle has reached its melting point no heating takes place any more. Instead, an equation has to be implemented that calculates the proceeding phase transition. The available heat flux was again calculated via 5–15. The change in mass was then determined on basis of the following equation:

$$m_{s,t+1} = m_{s,t} - \frac{\dot{q}}{\triangle H_{fus}} * t \tag{5–18}$$

5.3.1 Comparison of results in Matlab and OpenFoam

In the Matlab® model melting starts at $t = 0.00025\ s$ and is completed at $t = 0.01854\ s$ which is shown in figure 14. The corresponding time-dependent profile of solid mass fraction can be seen in figure 15. In OpenFOAM® melting starts at around $t = 0.00017\ s$ and ends approximately at $t = 0.013\ s$.

It is believed that the melting process is faster as OpenFOAM® considers gas flow around the particle that increases the heat transition coefficient α through the Ranz-Marshall correlation. The resulting temperature and mass fraction profiles look physically plausible and realistic and also the time ranges for melting fit together well taking into account the different approaches to the problem. The relative derivation between both processes in terms of time is around $30\ \%$ which might be a bit high but is difficult to evaluate quantitatively. For a better accordance of both data sets a closer look at initial settings for the turbulent parameters could have possibly helped. Generally, the outcome of the melting particle test turned out to be satisfying as it could be shown that the particle behaviour is displayed quite similar for both approaches.

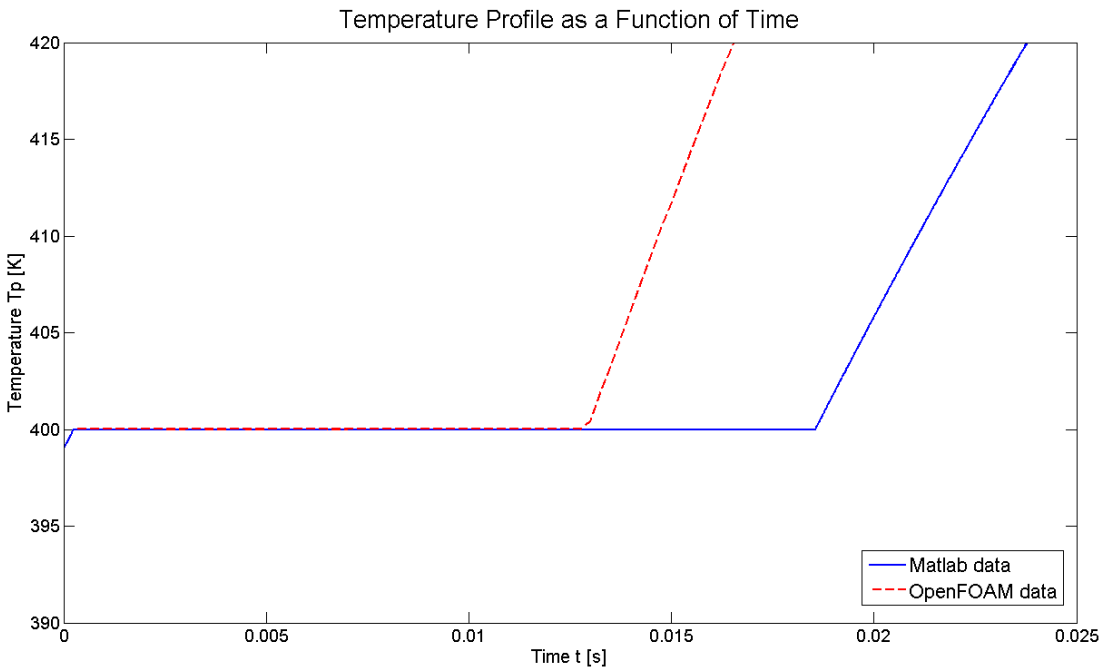

Figure 14: Temperature profile for the melting particle in the simplified test case of Matlab®

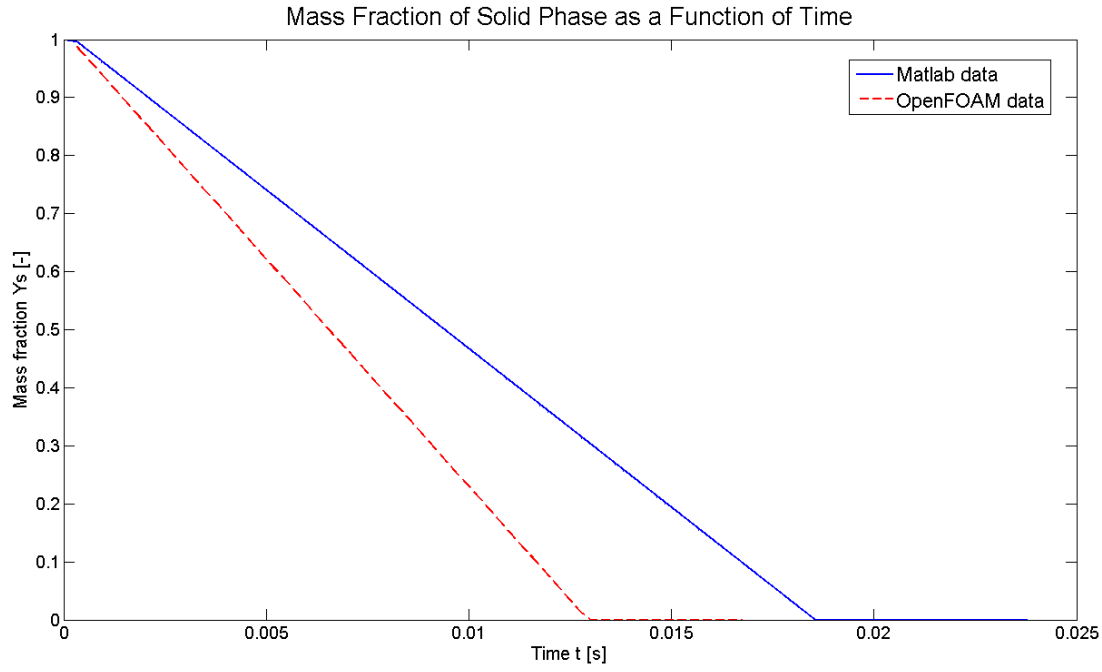

Figure 15: Mass fraction of solid phase as a function of time in the simplified test case of Matlab®

5.4 Mass Conservation for Melting Particles

A problem that occurred for the simulation of melting particles was that the composition of the gas phase did not comply completely with mass conservation. More precisely, summing up all mass fractions of the gas phase returned a value above one. In the test case this behaviour was not noticed as it was somehow related to the number of particles in the system and only occurred in cells where melting particles were present. The type of error was rather surprising as the particles did not contribute mass to the carrier phase in terms of a mass fraction Y_{melt} but somehow influenced the amount of other gases regarding a total mass fraction unequal to one. For example could be observed that during the melting process the percentage of present oxygen and nitrogen in the cell both increased over the initially introduced values. At the beginning this deviation was in the range of percent and increased with every time step where melting took place. Yet, the same solver was used as for evaporating particles with source terms in all continuity equations although no mass transport took place. For this reason the first thought was that the problem could be solved by removing the source terms for melting particles from the mass transfer related equations. This did not lead to the desired success so further investigations had to be made. As a second countermeasure the solution of Y and p in the case settings was refined which generally improved the stability and the impression of the solution for example concerning the homogeneity of the displayed pressure field but could not satisfactorily decrease the error in mass conservation. At the end, the quantity that was responsible for transmitting information concerning mass transfer from the Lagrangian to the Eulerian phase could be found and was disabled. This proceeding helped to reduce the deviation to the third decimal digit and kept it small over the whole simulation time.

6 Determination of the Necessary Ignition Energy

The Ignition Energy for different case set-ups was determined in a model displaying a cylindrical three-dimensional cut-out of the modified Hartmann tube. More precise, the considered section displays the immediate surroundings of the introduced electric spark. As only the ignition was of interest the geometry had a length of $6\ mm$ and a diameter of $16\ mm$ as shown in figure 16. It was already checked concerning mesh independency by Pollhammer [1].

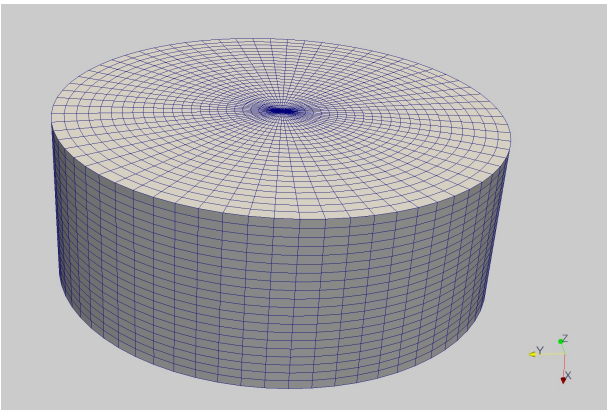

Figure 16: Cylindrical cut-out of a modified Hartmann apparatus used for the determination of the Ignition Energy

In order to get comparable results, all cases were run with an inert additive concentration of $750\ g/m^3$ and with particles of the size of $50\ \mu m$, $30\ \mu m$, $20\ \mu m$ and $15\ \mu m$.The evaporating as well as simple inert particles have a fixed density of $\rho = 2200\ kg/m^3$ and a heat capacity of $c_p = 900\ J/kgK$. For the melting particles the properties were set to $\rho = 2300\ kg/m^3$ and $c_p = 2000\ J/kgK$.

Principally the value is found by an approximation that is aimed to reduce the energy range in which the is located step by step. If neither indications nor experiences exist it can sometimes be time-consuming to find the value for a specific case set-up. By interpreting the outcome of

a specific ignition test a good estimate can be made for a next, more accurate try. If a lot less energy is introduced into the system than necessary for a self-sustaining flame front, the system cools down very fast again. The longer regions of hot temperatures can persist the closer is the Ignition Energy. Figure 17 shows the introduction of a $28\ mJ$ electric spark into a system with $28\ \mu m$ inert additives of $750\ g/m^3$ that is very close to an ignition.

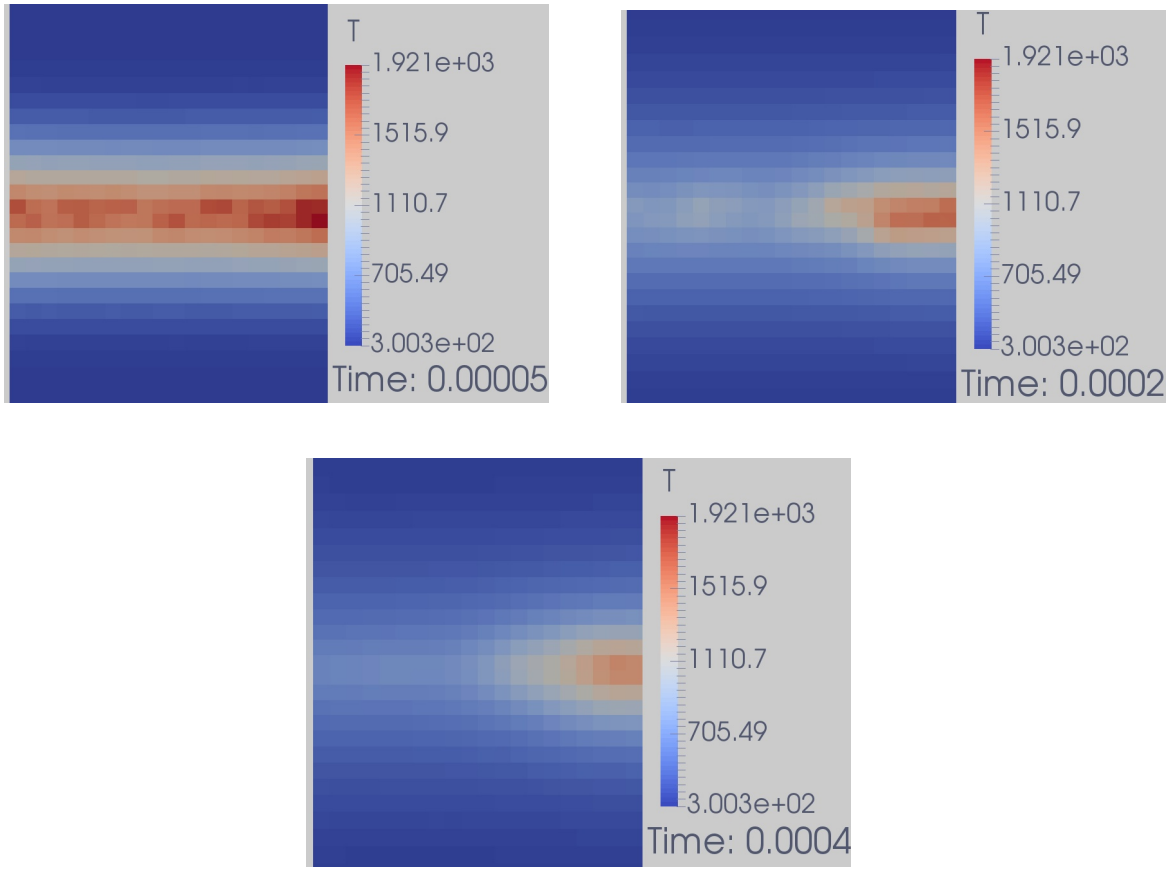

Figure 17: Introduction of energy from an electric spark that nearly leads to an ignition of the flammable dust/air mixture coloration in temperature $[K]$

On the opposite side, big areas of high temperatures in the very initial phase of a combustion are a sign of too much energy input as can be seen in figure 18 where a lycopodium/air mixture is ignited with $28\ mJ$ instead of the necessary $25\ mJ$. If the introduced spark nearly reaches the minimum value only one or two point sources start a delayed combustion process. Figure 19 shows such an ignition for a system containing simple inert particles in a concentration of $1500\ g/m^3$. The same effects as described in this section were also observed in [1].

In laboratory experiments the ignition energy is not assigned to a specific value as random behaviour of the ignited mixture influences this value significantly. To reduce computing effort and save time the ignition energy was determined as the mean value between an energy input that was able to ignite the mixture and one that was not. For the most cases they stretched over an energy range of $2\ mJ$.

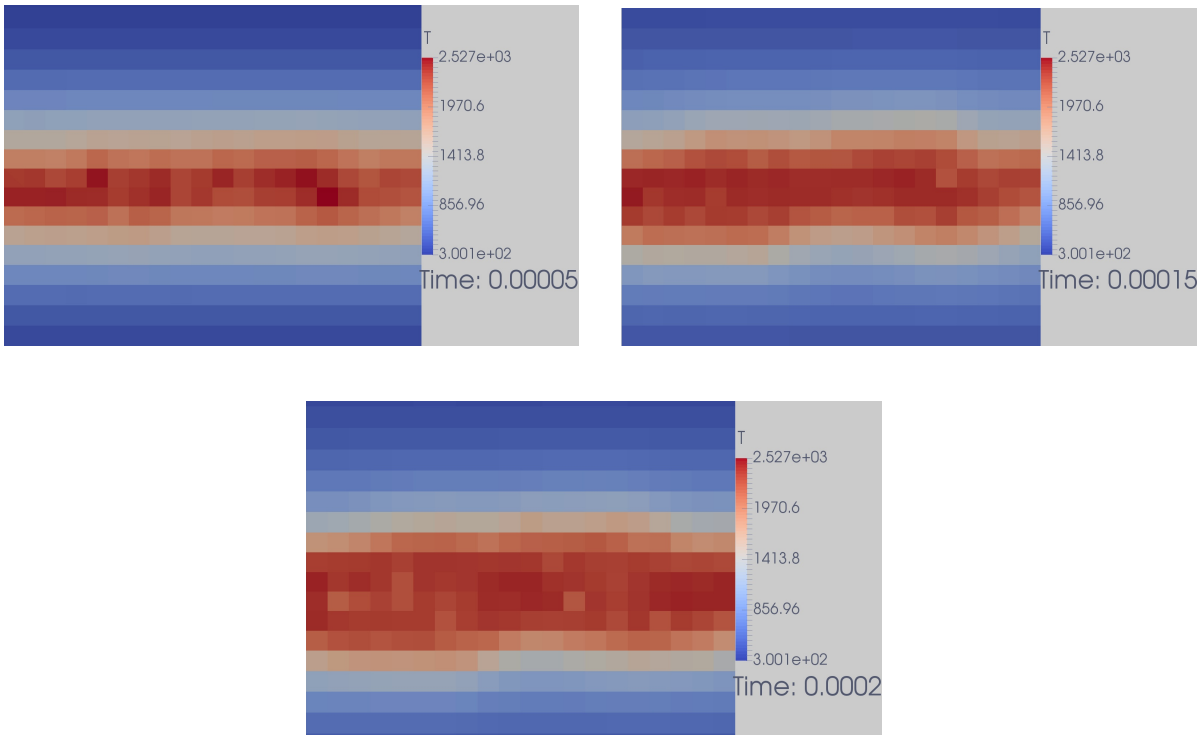

Figure 18: Introduction of energy from an electric spark that is considerably higher than the ignition energy; coloration with temperature $[K]$

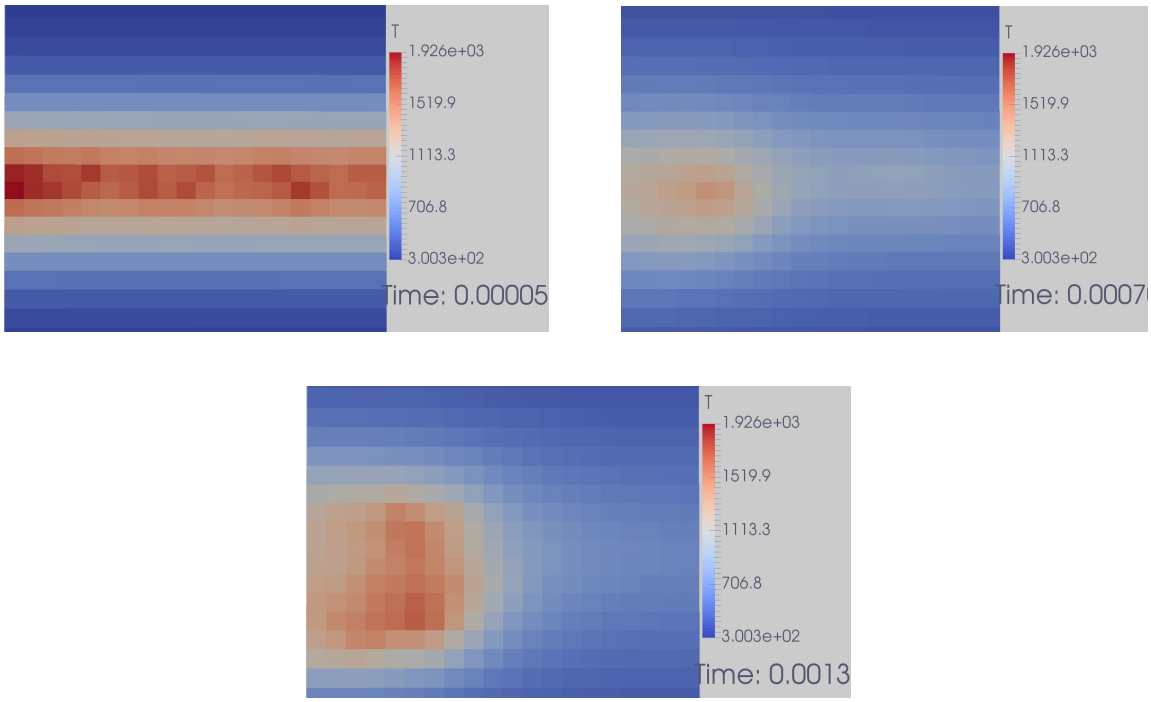

Figure 19: Introduction of energy from an electric spark that corresponds to the Ignition Energy; coloration with temperature $[K]$

6.1 Resulting Ignition Energies

Table 5 shows the resulting ignition energies that were determined for each material/particle diameter combination for a consistent concentration of $750\ g/m^3$. In figure 20 the graphical comparison of the outcome is shown. By decreasing the uniform diameter of the particles one can observe small increases of the ignition energy. Between the smallest and the biggest size the number of particles rises more than 37 times leading to an augmentation of around $5\ mJ$ for inert particles and lies in the same range for the other used additives. In contrast to the priorly expected outcome the size reduction of simple inert particles is able to increase the ignition energy on a value higher than both other tested additives that show additional heat sinks. Obviously, the variation of the diameter is not changing their effectiveness as a suppressant remarkably. In section 7.2.4 a possible explanation for the poor performance of melting particles regarding the increase of the ignition energy is given. It states that the decrease of reaction rates leads to a slowed down proceeding of the flame front that in turn can sustain the combustion process as more time is available for diffusion. Water-laden particles show completely complementary behaviour as the vapour seems to push the combustion zone forward. Indeed, results described in 7.2.2 indicate that the evaporation of water is too slow for being a competitive process besides the combustion. Smaller particles are physically not able to change this fact as still the same amounts of heat are necessary for vaporisation of water. It is expected that the decreased ignition energy that is observable in those systems can be derived from the release of vapour that is assumed to influence the turbulence in the gas phase enhancing.

The gathered results for the Ignition Energies imply that the capacity of a heat sink plays a subordinate role for the suppression of combustions in flammable dust/air mixtures. The choice of $15\ \mu m$ instead of $50\ \mu m$ simple inert particles has a bigger effect on the ignition energy than the application of melting particles as can be seen in table 5. In chapter 7 will be shown that the influence factors for the ignition energy and flame propagation velocity differ significantly from each other and that better thermal properties may not play a role for the first but nevertheless for the second safety index.

Table 5: Results of simulations aiming to determine ignition energy for different types of additives and varying particle sizes)

Type of Additive/Size	-	$50\ \mu m$	$30\ \mu m$	$20\ \mu m$	$15\ \mu m$
No Additives	$25\ mJ$				
Simple Inert Particles		$25\ mJ$	$26\ mJ$	$29-30\ mJ$	$29-30\ mJ$
Water-laden Particles		$17\ mJ$	$17\ mJ$	$27-28\ mJ$	$25\ mJ$
Melting Particles		$24\ mJ$	$24\ mJ$	$25\ mJ$	$25\ mJ$

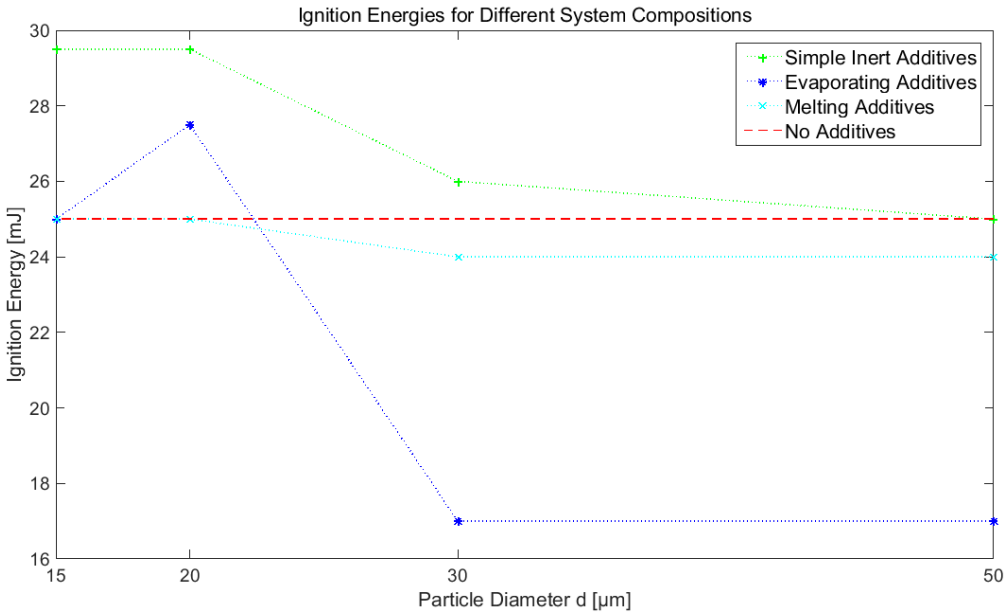

Figure 20: Graphical comparison of the necessary ignition energies for different system compositions

6.2 Release of Combustion Heat as a Function of Time

In section 3.3 is described how the source term, in which the heat of combustion is contained, can be transferred to a recordable volume scalar field. The term only contributes a value to the energy equation as long as a reaction takes place in the gas phase. Plotting the value over time, it shows the profile of energy input due to reaction. Included in the value of released heat is the rate at which the educts are converted to products. Therefore it can be used for depicting the ongoing reaction process. In 7.1 is described how the same quantity is resolved along the space coordinate z in order to determine the flame propagation velocity. In contrast to this, the plots in figure 21 display a total value for the complete geometry. Besides the red one (solid line) that contains data of the system with no additives, each of the depicted graphs belongs to a system of $50\ \mu m$ additives in a concentration of $750\ g/m^3$. To ensure that all mixtures can actually ignite the modelled spark was set to a value of $28\ mJ$. Considering the area below the graphs it can be seen that in different systems slightly variable amounts of reaction heat are released. A reason for this might be the temperature dependent reaction enthalpy but also that particles are pushed out of the geometry due to the formed pressure wave and thereby control the amount of available fuel for combustion.

A few time steps after the ignition of a dust/air mixture in the presence of melting particles the propagating flame front stagnates completely. For this reason it is not shown together with the other results.

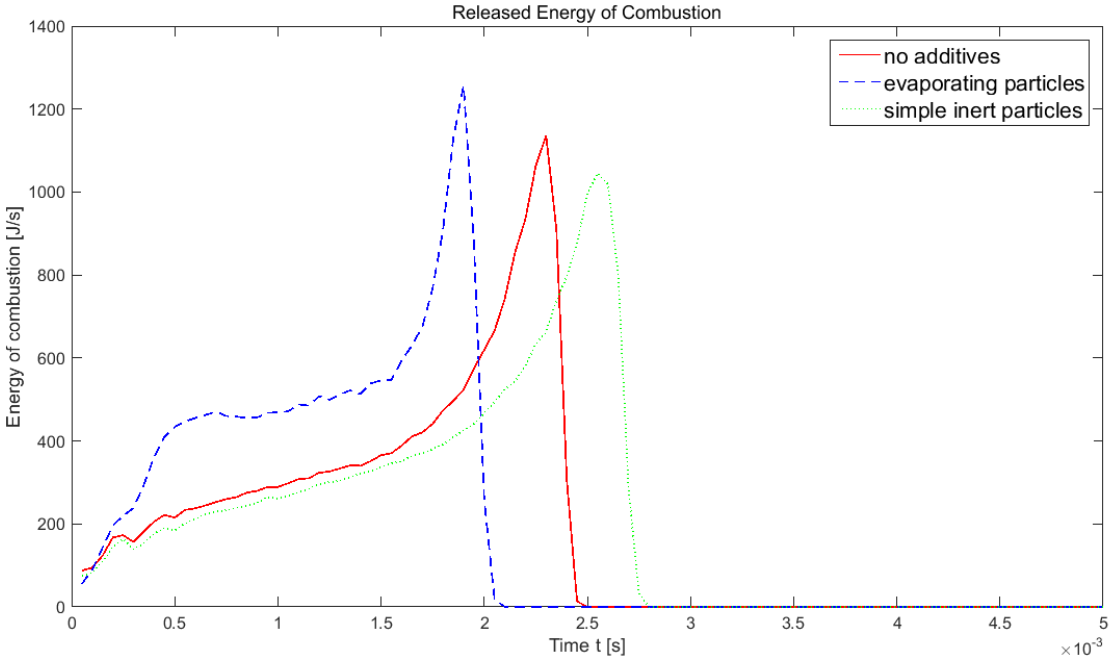

Figure 21: Released Energy of Combustion (flux) $[J/s]$

6.2.1 Propagating Combustion in a Flammable Mixture Containing Water-Laden Particles

In the very early phase of ignition, hot zones can only be found close to the electric spark. As a consequence of temperatures over $10.000\ K$ the sudden volume expansion in the gas phase leads to a pressure wave that reduces particle concentration in those regions. The presence of fuel at that time is limited and its concentration is believed to control reaction rates besides diffusion. The blue graph (dashed line) implies that the combustion already starts very fast in a system containing water-laden particles. As those particles differ from other particulate additives only through their mass transfer into the gas phase it is reasonable to presume that the observed effect can somehow be related to the sudden release of vapour. It is believed that the setting free of vapour acts promoting for the combustion by improving the mixing conditions on molecular scale and also by supporting the natural propagation of the flame front in regions with unconverted oxygen and fuel. Especially in the first few time steps this is advantageous for developing a stable reaction process.

In order to support the theory the turbulent conditions in the first few time steps were examined. The most important variables of the $k-\epsilon$-model are dissipation, turbulent kinetic energy and turbulent viscosity. In the considered model k and ϵ are assumed to be in a local equilibrium which means that they contain the same values. A problem that applies equally to all of them is the fact that only volume integrated values can be written out easily in post-processing for further investigations. As a consequence a lot of informative data is lost and replaced by an average for

each time step. Turbulent viscosity μ_t is a very useful quantity for expressing the dependency of reactions on turbulent mixing but as it is a function of the local conditions it does not make sense to consider a mean value of it. Therefore it was decided to display the turbulent kinetic energy over the first few time steps as shown in figure 22. Again the blue graph (dashed line) displays the behaviour of the case in which water-laden particles were introduced. It can clearly be seen that during the first few time steps more turbulence is present than in the other cases that were all ignited with $28\ mJ$. The more advanced the time step is, the less informative becomes figure 22. This is due to the fact that the flame fronts do not proceed simultaneously and the comparison of one time step displays each combustion in its individual stage. Additionally, the ongoing decrease of turbulent energy in the presence of water-laden particles even below the level of simple inert particles and no additives does not mean that in its combustion zone less turbulence can be found. It is rather an expression of the cooling down effect directly behind the flame front that reduces temperatures and thereby flow velocities in this region.

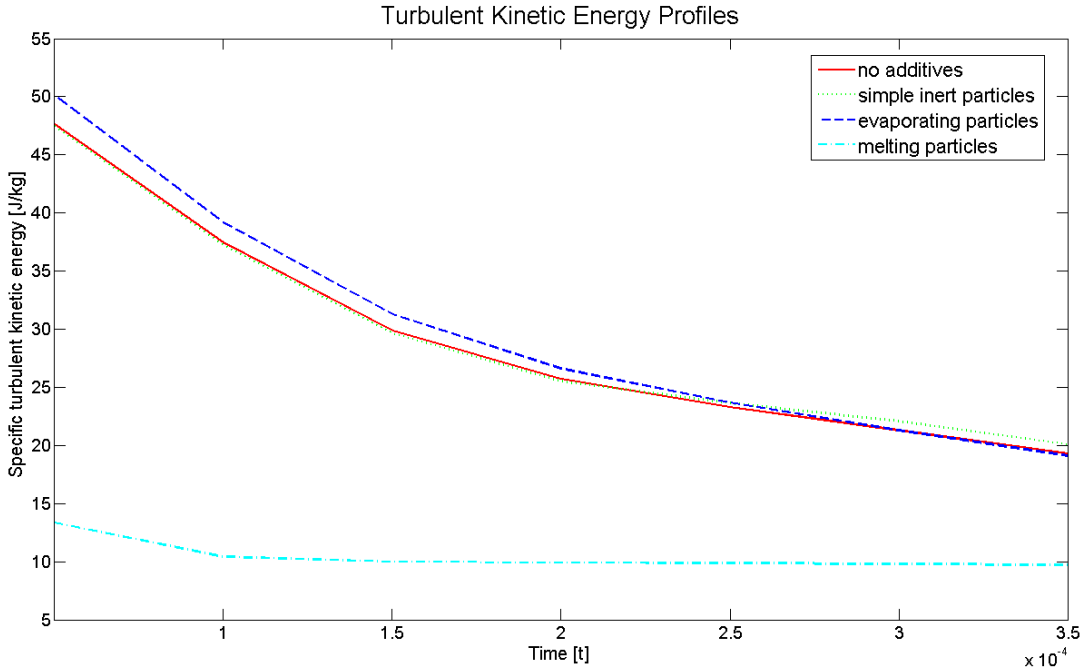

Figure 22: Comparison of the specific turbulent kinetic energy $[J/kg]$ of the gas phase for the four different system set-ups

The second effect that has been mentioned can be well observed when displaying the oxygen mass fraction in the gas phase over some time as can be seen in table 6. In an advanced explosion process the combustion takes place only within a small cylindrical stripe. Shortly after ignition the complete volume of the previously introduced electric spark forms a reaction zone and persists as long as oxygen is present. For explosions in most flammable mixtures it sustains only over a few time steps ($< 0.5\ ms$) and does not proceed in space remarkably as the reaction

in its center consumes oxygen faster than it can propagate into unburned regions. For a system containing water-laden particles the behaviour is different as the vapour is believed to push the reaction zone forward. Thereby the available reaction zone increases and the combustion generates higher heat flows than the other observed systems within the first few time steps. As soon as the flame front has its final appearance, the heat flux due to combustion shows similar gradients as the lycopodium/ air mixture with and without inert particles. The slight, nearly linear growth afterwards is expected to be a result of the increasing diameter of the cylindrically shaped flame front. The strong increase at the very end of the graph can be seen for all mixtures and is due to the acceleration of the flame front with proceeding combustion. The point when the source term reaches zero describes the time step where the flame front has left the geometry completely.

Table 6: Comparison of the ignition behaviour on basis of the oxygen mass fraction $[-]$

Inert particles	Water-laden particles	Melting particles
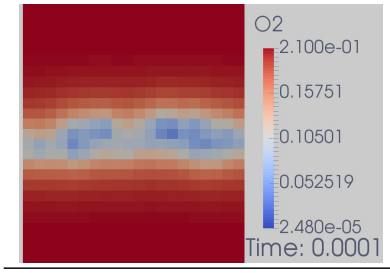	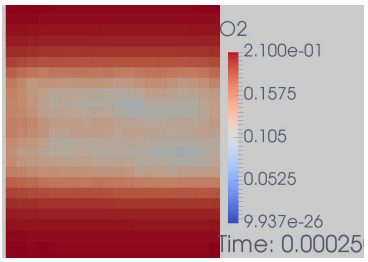	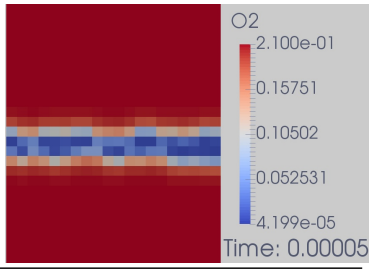
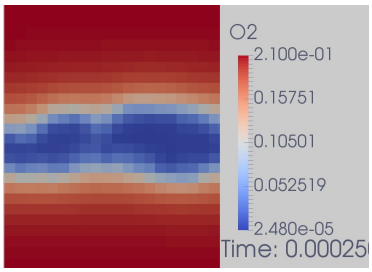	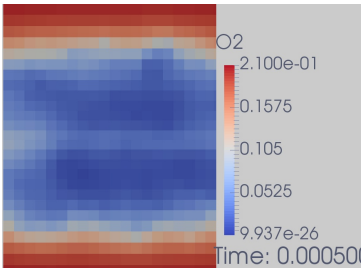	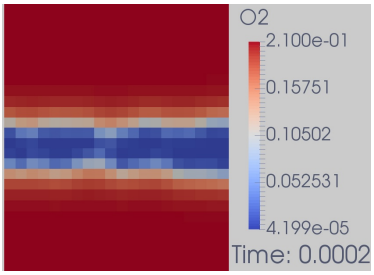
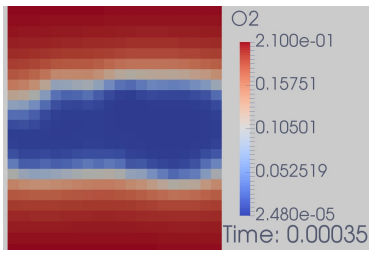	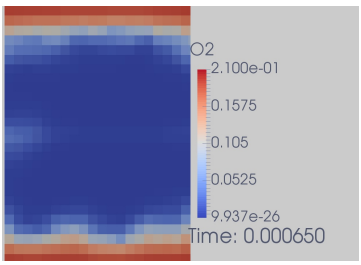	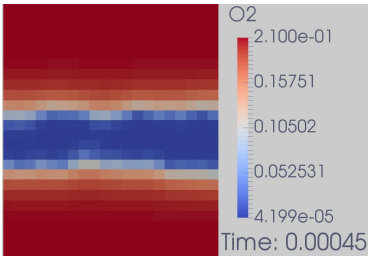

6.2.2 Propagating Combustion in a Flammable Mixture Containing Simple Inert Particles

Basically, the profile of heat flow due to combustion for simple inert particles (dotted line) looks similar to the one for water-laden particles. However, the transition between the first

steep gradient and the following slight increase of heat flux takes place much earlier and can be explained by the fast development of the final state of the flame front that limits the size of the reaction zone and thereby its heat input. In the initial phase and also during the first millisecond of linear growth the observed graph fits together very well with the lycopodium/air mixture without additives (solid line). With proceeding time the red graph (solid line) shows a steeper increase than the green one (dotted line) that is is due to different flame propagation velocities. In the system with simple inert particles the three-dimensional flame propagation shows a very inhomogeneous shape for the first few time steps until a cylindrical flame front can develop which additionally retards the the proceeding of the combustion.

6.2.3 Propagating Combustion in a Flammable Mixture Containing Melting Particles

The combustion in flammable dust/air mixtures that contain melting additives proceeds very slow, even not to say nearly ceases. Under these conditions the investigation of the propagating combustion does not provide a lot of information about the temporal development. For this reason a higher concentration of flammable dust namely $1800\ g/m^3$ was tested additionally to see how melting particles influence the combustion energy profile with time. As can be seen later in section 7.2.4 the heat of combustion that is released in systems containing melting additives is primarily consumed by the heat of fusion. As the flow in the observed geometry is caused solely by natural convection the decreased temperatures lead to lower turbulence and hence to bad mixing conditions. In accordance with Sutherland the decreased temperatures decline molecular diffusion which is also expected to be the reason why reaction zones in those systems are observed to be much thicker than in the others. In contrast to the other reaction profiles displayed in figure 21, that all show very steep gradients at the end, the combustion in presence of melting particles shows a rather homogeneous increase of combustion energy up to the final maximum (figure 23).

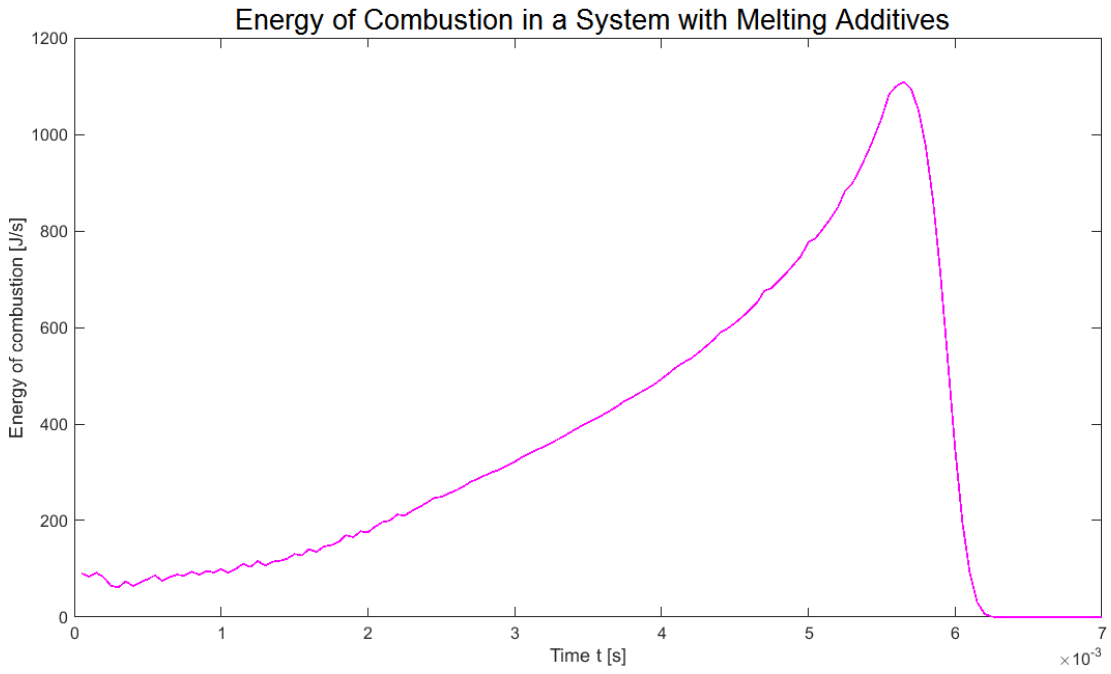

Figure 23: Released Energy of Combustion (flux) $[J/s]$ in a system containing melting particles

7 Investigating Flame Propagation in a 2D Pipe Profile

The second characteristic value for dust explosions that is examined within this thesis is the flame propagation velocity which is determined for all three different types of inert particles and the plain lycopodium/air mixture. The geometry used for the ignition energy is not suitable for this task as it is firstly too small and secondly not displaying vertical propagation well enough. Another problem raising with the choice of geometry is the dependency of the flame propagation velocity on shape and dimensions. A common apparatus used for experiments that aim to record the proceeding flame front is the modified Hartmann tube described in 2.1.1. In order to be able to assess the findings with experimental data it was decided to use this geometry as a basis for the CFD-model. The tube has a height of $32\ cm$ and a diameter of $8\ cm$.

It was planned to derive the propagation velocity by tracking the location of the proceeding flame front. For this purpose the resolution had to be high as it was important to have a well defined delimitation between the actual combustion zone and its surroundings. Calculating the flame propagation on a 3D geometry with the specified dimensions requires rather high computing performance and several days to complete which is undesirable especially when several cases have to be modelled. A very good solution for this problem is using a 2D cross section of the tube as shown in figure 24a. This way no three dimensional effects can be observed but the vertical movement of the flame front can be displayed very well. In this thesis no mesh independency study was carried out but in [1] a similar geometry with slightly different measures and same cell size was checked by this regard. The combustion is started by introducing a circular hot zone in the lower part of the geometry with stoichiometric gas composition. For both particle types, lycopodium and inert additives, the diameter was set to $50\ \mu m$ to keep the number of particles small. The particle concentrations were chosen to be in the magnitude of the cell number. This constitutes only a thumb rule to ensure that average cells contain one to two particles. High particle concentrations have a negative influence on the computing velocity and may cause problems due to big source terms they generate in small cells, while low concentrations can lead to flame extinguishing.

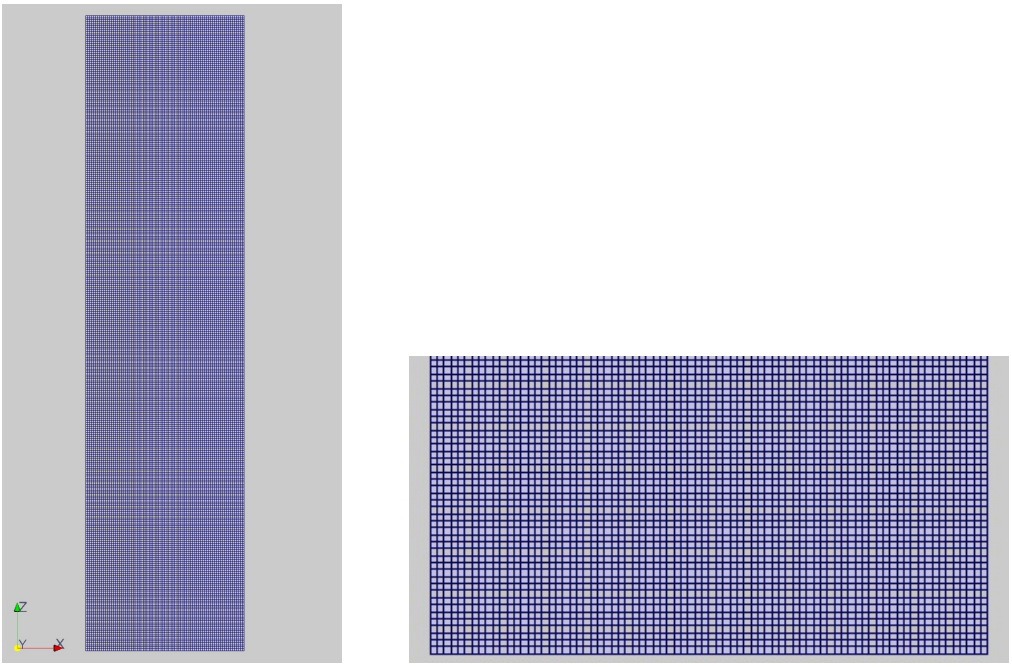

(a) Geometry as a whole

(b) Enlarged section;
cell size $1\ mm\ \times\ 1\ mm\ \times\ 1\ mm$

Figure 24: Vertical cross-section of the Hartmann apparatus used for the determination of the Flame Propagation Velocity

7.1 Calculation of the Flame Propagation Velocity

The flame propagation velocity is calculated in a post-processing step. Basically it is determined by tracking the proceeding flame front through the geometry and by localizing its position over time. Depending on which position in the flame front is considered the velocities vary significantly. As a characteristic value only the maximum flame propagation velocity is of interest. Due to the dome-shaped flame front the most advanced position and simultaneously the maximum velocity in z-direction is located approximately on the vertical symmetry axis of the tube. Two parameters that are written out for each time step proved to be particularly suitable for localizing this position.

The first option is the CO_2-content in the gas phase that creates a very well defined steep gradient separating the area before and behind the flame front. Plotting it over the tube length creates a S-shaped function similar to a cumulative curve as can be seen in figure 25. The second option is to choose the combustion source term that forms a peak in the combustion zone that is a few cells thick. The associated graph looks similar to a distribution curve (figure 26).

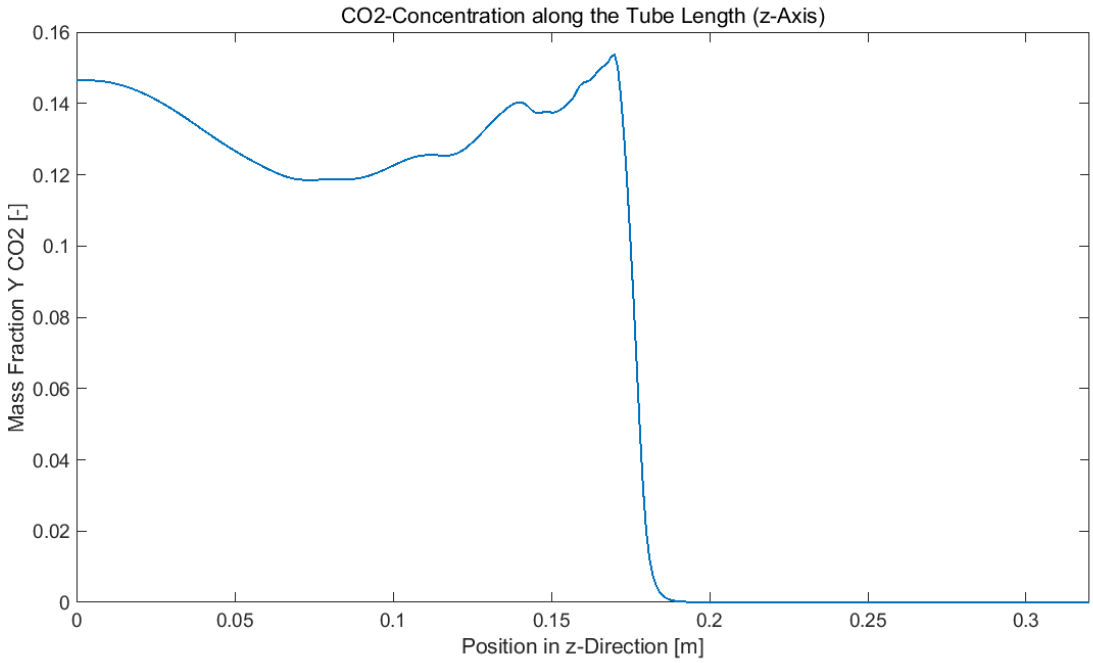

Figure 25: Examplary diagram displaying the CO_2-content in the gas phase along the vertical symmetry axis for one time step

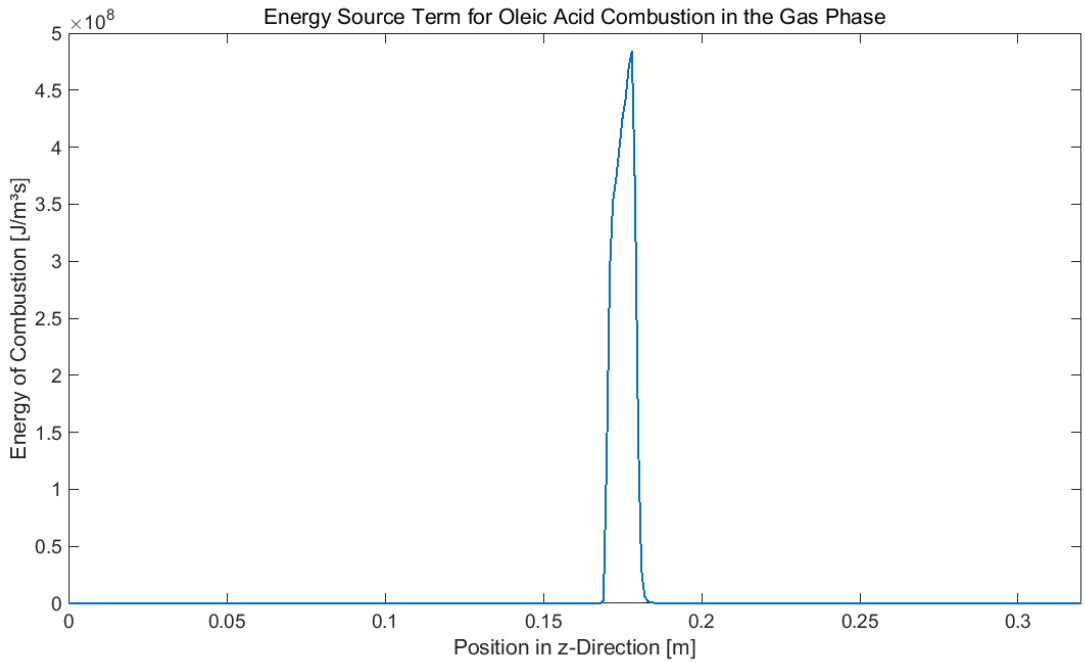

Figure 26: Examplary diagram displaying the combustion source term along the vertical symmetry axis for one time step

Regarding the combustion source term one can instantaneously derive the propagation velocity by determining the peak locations of two consecutive time steps in Matlab®. For the CO_2 the procedure is similar, though in this case the maximum gradient is tracked. For the post-processing both approaches were used to compare the results. The CO_2 content turned out to be more reliable than the combustion source term which did not always display the complete function course correctly.

7.2 Evaluation of Results

7.2.1 Flame Propagation Velocities (FPV)

In figure 27 the z-position of the flame tip is plotted over time. The blue graph (dashed line) covers the case carried out with evaporating particles, the red one (solid line) can be assigned to the original system with no additives and the green one (dotted line) displays the behaviour of a system with simple inert particles. The initial phase shows for all of them an approximately linear flame propagation. For the system containing simple inert particles this behaviour maintains up to very advanced times as can be seen in figure 28.

Figure 27 shows that the flame tip is not proceeding evenly. Physically this is a sensible phenomenon evoked by the heterogeneous composition of the system, more precisely due to random particle distribution, varyingly good mixing of oxygen and fuel and mutable temperatures. Besides this natural effect the numeric approach for calculating the velocities is partially responsible for the observed behaviour. As a consequence the numeric deviation of the z-position with respect to time results in a strongly swinging function course displaying the flame propagation velocity. As only the proceeding of a quantity from one cell to the other can be detected small time steps and big cell sizes can lead to false results. Due to reasons of computer performance the cell size is difficult to decrease but the time difference that is used for numerical differentiation can be increased. By augmenting the time steps for the calculation (not for the solution) one can reduce the number of peaks. As all the gathered data is used, there is no loss of information for the first time steps. Only at the end of the pipe at very advanced times the maximum velocities that are reached cannot be displayed properly as their values are not used any more. They were therefore determined separately using smaller time steps.

Generally all three velocity functions show an increase of the flame propagation velocity with progressing height which can also be seen in figure 28. The flame front in the system that contains vapour emitting particles reaches the end of the geometry first, followed by the inert additive-free system. At last and with remarkable retardation the reaction zone of a mixture containing simple inert particles passes the boundary of the considered pipe section. The evaporating particles cause a fast flame propagation in the pipe from the very beginning, increasing its velocity steadily up to a value of $18\ m/s$ at the end of the pipe. This outcome was

not expected as water was initially introduced as an additional heat sink that should extend the capability of particles to remove energy from the combustion zone. Instead, the presence of water-laden particles even accelerates the flame front.

However, the maximum calculated velocity is reached by the system containing no additives and constitutes $26\ m/s$. The flame propagation velocity that is determined for the case where inert particles are implemented, stays constant for a long time and only within the last few centimetres increases to a maximum of $11\ m/s$. The reason for this is that due to the pressure wave that accompanies the flame front, particles are escaping through the upper opening of the pipe and cannot slow down the propagation any more.

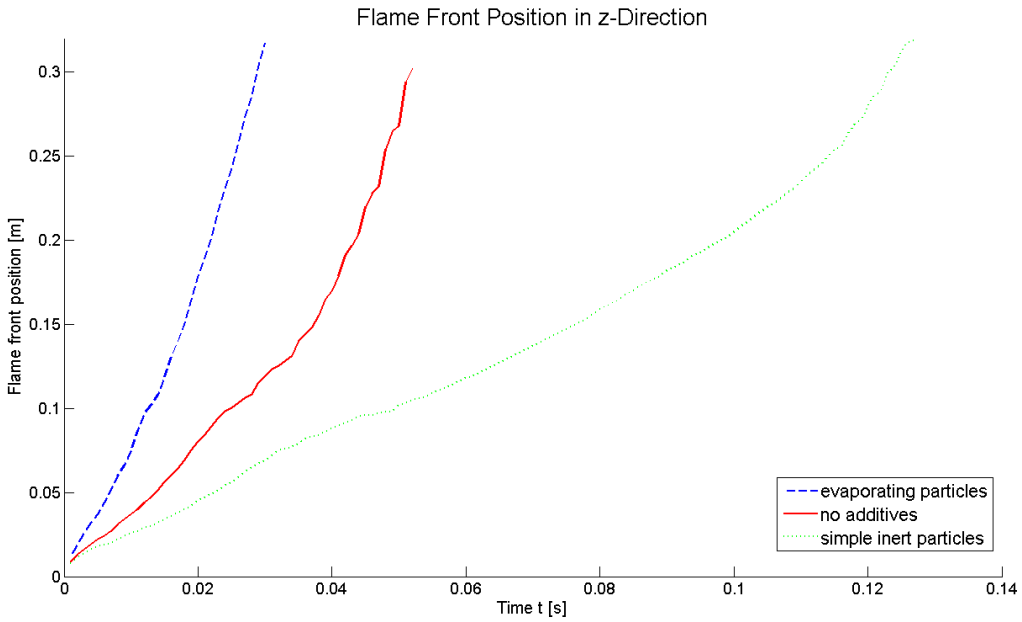

Figure 27: Flame front positions over time for three different systems

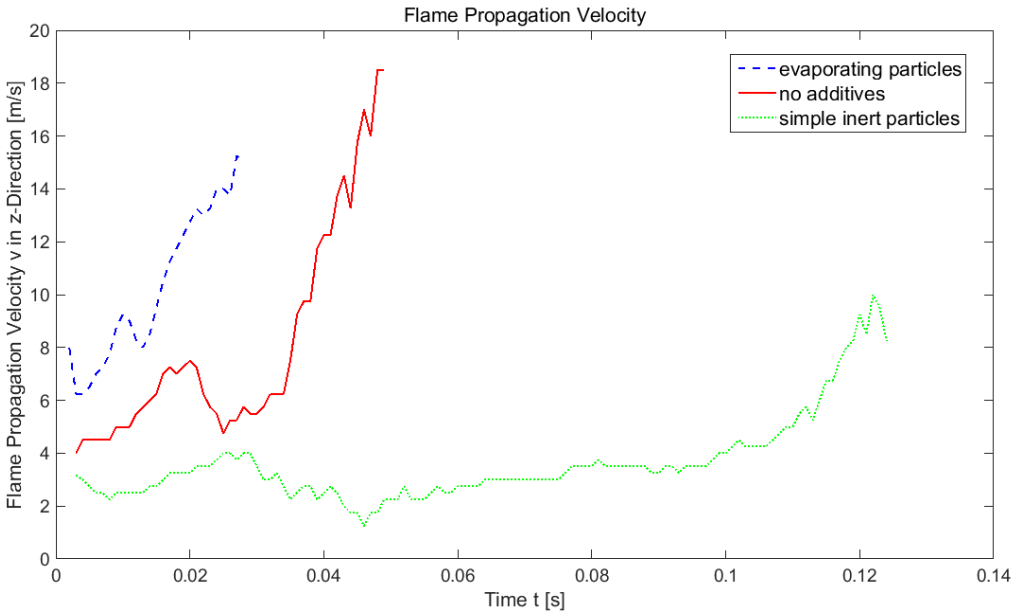

Figure 28: Flame propagation velocity derived from the flame front positions over time for three different systems

7.2.2 Behaviour of Water-Laden Particles in the Ignited Lycopodium-Air System

The third column in table 7 depicts the combustion process with evaporating particles as additives. The sequence of graphics shows 4 different stages of the explosion at different time levels. Several distinctions compared to the other systems can be seen on the spot. The flame fronts, besides the one displayed in the last graphic, are nearly perfectly dome-shaped and show all only a very thin layer at the very top that is acutally a hot region. Having a look at the volume scalar field of combustion source term one can see that the reaction takes place solely in this very small stripe (figure 29a). The combustion is limited by availability of oxygen that is already completely consumed behind the flame front. Obviously the reactions in the small stripe is suffiecient for the complete conversion of oxygen.

When displaying the H_2O content of the inert particles after ignition it can be observed that effective evaporation takes place only after the flame front has passed. This is due to the fact that the resistence of lycopodium particles against heating-up and phase transition is lower than for water-laden additives. The high heat capacity and evaporation enthalpy makes the vapourisation of water in the system slow. For the volatilisation of $C_{16}H_{34}$ a rather low energy input is necessary initialising it already in front of the combustion zone (figure 29b). This effect has already been well investigated from Pollhammer [1]. Behind the hot region, the majority of lycopodium particles has already evaporated the whole quantity of oleic acid. Under this conditions the available thermal energy is used for the phase transition of water, cooling the system down very quickly (figure 29c).

This effect is very strong along a central stripe starting directly behind the hot zone and can

be explained by the inward movement of particles that is observable. A possible reason for this behaviour is that the expansion of gas near the walls causes a mass flow directed to the center of the pipe.

The vapour that is set free behind the flame front also leads to a sudden increase of mass in the gas phase pushing the combustion zone forward. In addition, the elevated temperatures lead to an expansion of volume and thus to a decreasing density in those regions. The hot gases rise and augment the previously mentioned effect. This effect occurs in all observed systems.

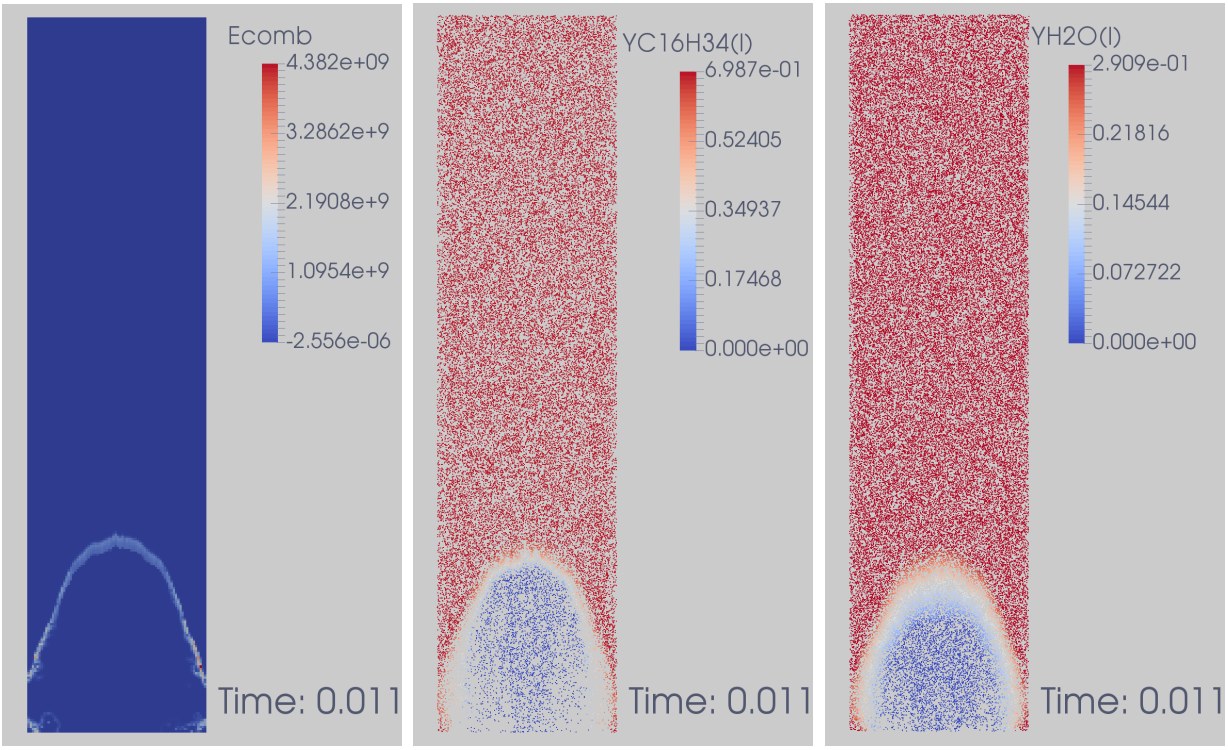

(a) Localisation of the flame front with vol. scalar field $Ecomb[J/m^3s]$

(b) $C_{16}H_{34}$-content $[-]$ of lycopodium particles

(c) Water content $[-]$ of inert particles

Figure 29: Quantities describing the combustion process in a flammable dust/air mixture containing water-laden additives

Besides these accelerating factors the complete reaction takes place faster in a system with water-laden particles added. Generally in all considered cases the reaction in the combustion zone is diffusion-limited which can be seen in figure 30b. While in all other systems the complete flame front is strongly dependent on the bad mixing conditions, the water-laden particles create a combustion zone that is at least in the regions left and right of the pipe center very well mixed. As can be seen in figure 29a the reaction zone is also very thin which is an additional indication for the theory that diffusion is not decreasing reaction rates so heavily as in the other systems. The thickness of the flame front is basically a phenomenon expressing how fast the available oxygen is converted into combustion products.

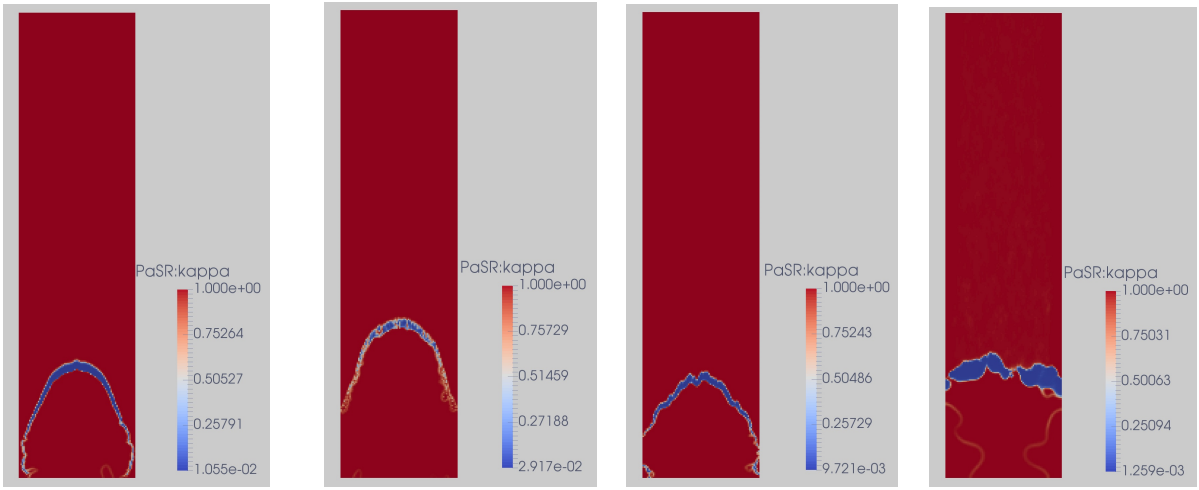

(a) Mixing parameter κ in a system with no additives at $t = 0.01\ s$

(b) Mixing parameter κ for a system water-laden additives at $t = 0.007\ s$

(c) Mixing parameter κ for a system with simple inert additives at $t = 0.0155\ s$

(d) Mixing parameter κ for a system with melting additives at $t = 0.515\ s$

Figure 30: Mixing parameter κ for the 4 different case set-ups at one specific one time step

Making a reaction faster is under these circumstances only possible by providing better mixing conditions, what in turn can only be obtained by increasing turbulence. It is therefore assumed that the accelerated reaction is result of the molecular movements initiated by the locally released vapour. In figure 31 the turbulent viscosity is displayed. According to the Boussinesq assumption it is related to the shear stress between the gas particles that is caused by turbulence. From this point of view, one can say that the higher the turbulent viscosity μ_t is, the stronger is the development of eddies and the better are the conditions for diffusion in the system. In figure 31a the turbulent viscosity in the boundary region of the walls is nearly double the maximum value of figure 31b. This outcome fits very well with the assumption that higher turbulence is the reason for the faster proceeding reaction that can be observed in systems with water-laden additives. To conclude, it is expected that all three previously mentioned effects play a more or less important role in the speed-up of the flame front. However, quantifying their actual contribution is very difficult and further investigations on this topic would have gone beyond the scope of the thesis.

7.2.3 Behaviour of Simple Inert Particles in the Ignited Lycopodium-Air System

The flame propagation in a mixture containing simple inert particles is very uniform and slow compared to the other compositions displayed in figure 28. The inert particles interact with the gas phase by removing heat that is set free during the combustion. As all other combustions in lycopodium and air, the reaction is diffusion-limited. This means that kinetic limitation due to decreasing temperatures is not playing a role for the combustion as it allows higher reaction rates than are actually achievable as a consequence of bad mixing. Figure 30c shows the mixing parameter κ that basically describes to what extent either kinetics or mixing have an impact on the proceeding combustion. Mathematically, the reaction rate is multiplied by a value taking into account the mixing behaviour on molecular level due to turbulence and is derived from variables

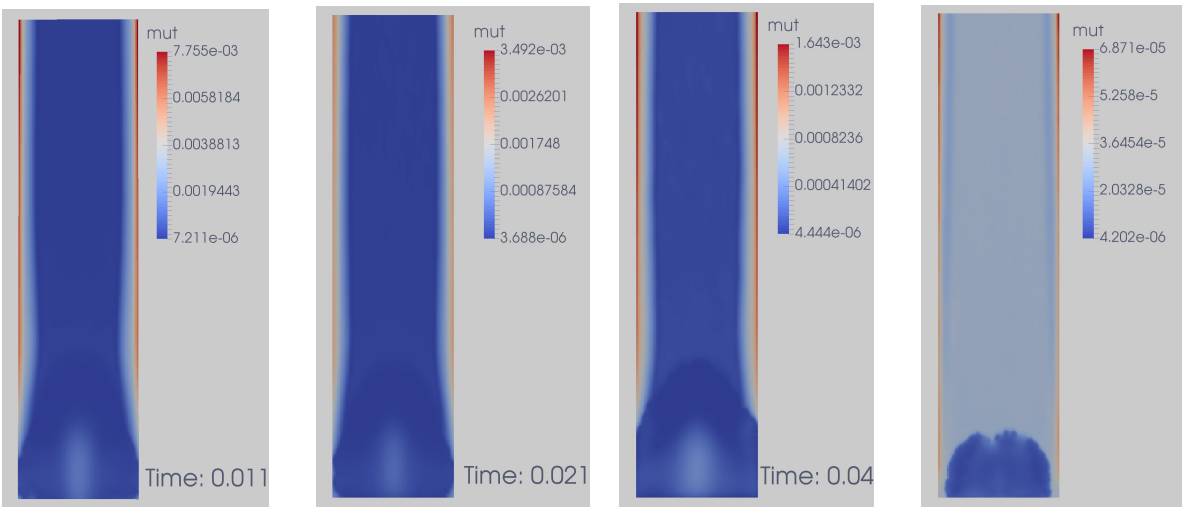

(a) Turbulent viscosity in a system with evaporating particles

(b) Turbulent viscosity in a system with no additives

(c) Turbulent viscosity in a system with simple inert particles

(d) Turbulent viscosity in a system with melting particles

Figure 31: Comparison of turbulent viscosity $\mu_t[Pas]$ for systems containing different types of extinction powders

associated with the $k-\epsilon$ model. Besides the reduction of turbulent diffusion the temperature decrease due to heat removal leads to slowed down molecular diffusion in the system which in turn leads to lower combustion rates.

A second effect that can be observed is the reduced turbulence resulting from the transport of turbulent kinetic energy from the Eulerian to the Lagrangian phase. It is assumed that this is a very important reason for the decelerated flame propagation. In figure 31c the volume scalar field of turbulent viscosity for one time step is displayed.

Theoretically, this behaviour should have been also observed for water-laden particles but the release of water vapour concealed this impact and superimposed a mixing process. The scales that are describing the turbulent viscosity μ_t quantitatively for the observed systems as displayed in figure 31 allow a principal comparison concerning turbulence. From this data it can already be seen that apparently turbulence is strongest with water-laden particles and weakest with melting particles. However, the simulation results from figure 31 look very similar which makes it difficult to see differences between the individual cases. Although figure 22 in section 6.2.1 used data of the ignition energy determination it is also very suitable in this case for showing that the advanced flame propagation in systems with water-laden particles is due to augmented turbulent mixing.

Table 7: Comparison of flame propagation with different additives

No additives	Inert particles	Water-laden particles	Melting particles
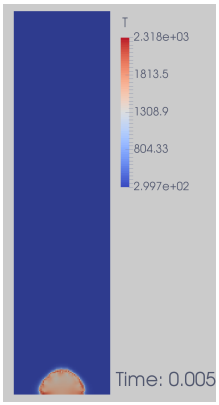	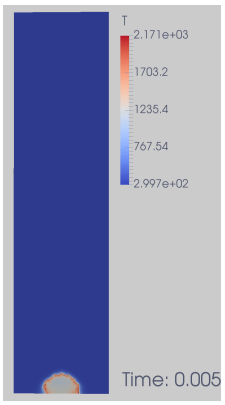	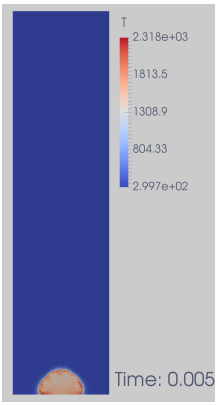	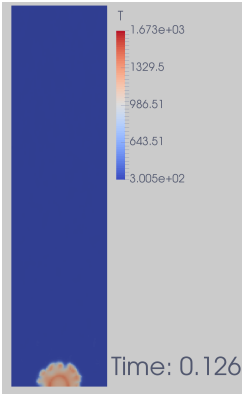
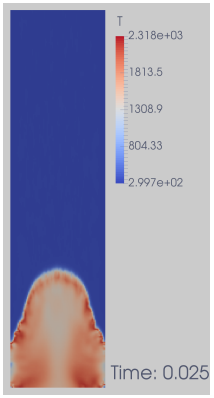	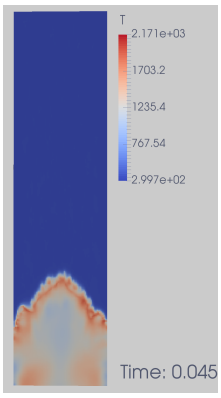	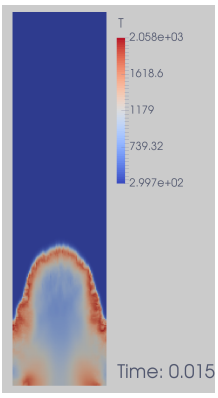	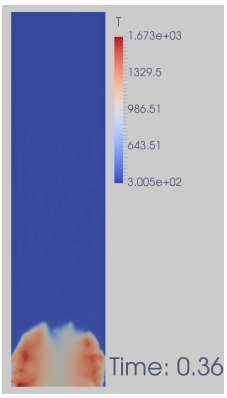
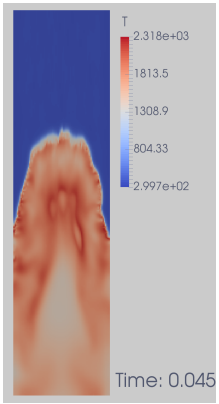	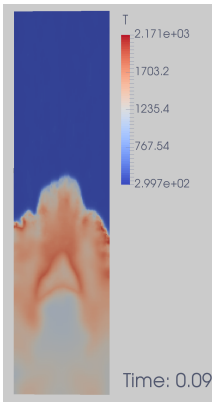	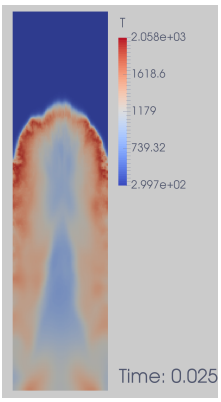	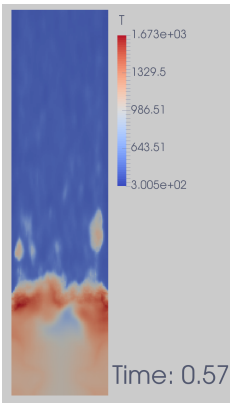
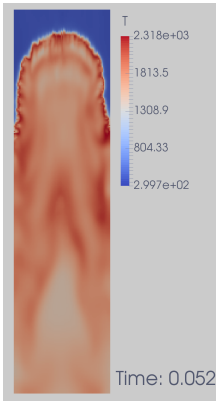	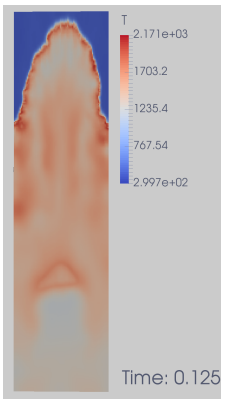	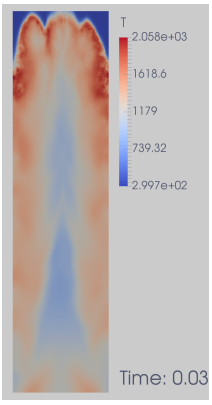	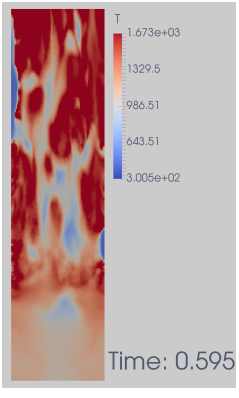

7.2.4 Behaviour of melting particles in the ignited lycopodium-air system

In a system where particles with low melting points interact with the combustion, the flame propagation practically ceases. For this reason the associated velocity could not be displayed with the other cases. For more than half a second the flame movement is limited to irregular expansions of the hot zone in the lower third of the geometry as can be seen in figure 32. Although the observed combustion is oxygen-limited, considerable amounts can still be found in a comparatively broad region behind the reaction zone. Obviously, the mixing on molecular level is very poor and prohibits higher reaction rates and faster flame propagation. The mixing parameter κ in figure 30d supports this theory and also the turbulent viscosity μ_t from figure 31d. Even in boundary regions where due to turbulence the reaction normally converges kinetic limitation diffusion is still the crucial process.

By using this type of additives it could be managed to make the heat absorption process competitive to evaporation and combustion of oleic acid. One can say that the behaviour of melting particles even exceeds a simple competitiveness as it constitutes the major heat absorption process as long as solid is available. For this reason it was possible to limit the release of fuel directly to the combustion zone and regions behind. This effect changes the propagation behaviour as the flame front is not fed from areas in front but instead from areas in the back. It is remarkable that despite of those adverse predominant conditions the flame is able to sustain itself. It is believed that the low buoyancy is responsible for the preservation of the flame front as it is obviously not strong enough to push the flame front forward in regions where no fuel is available. Figure 32 shows the associated simulation results.

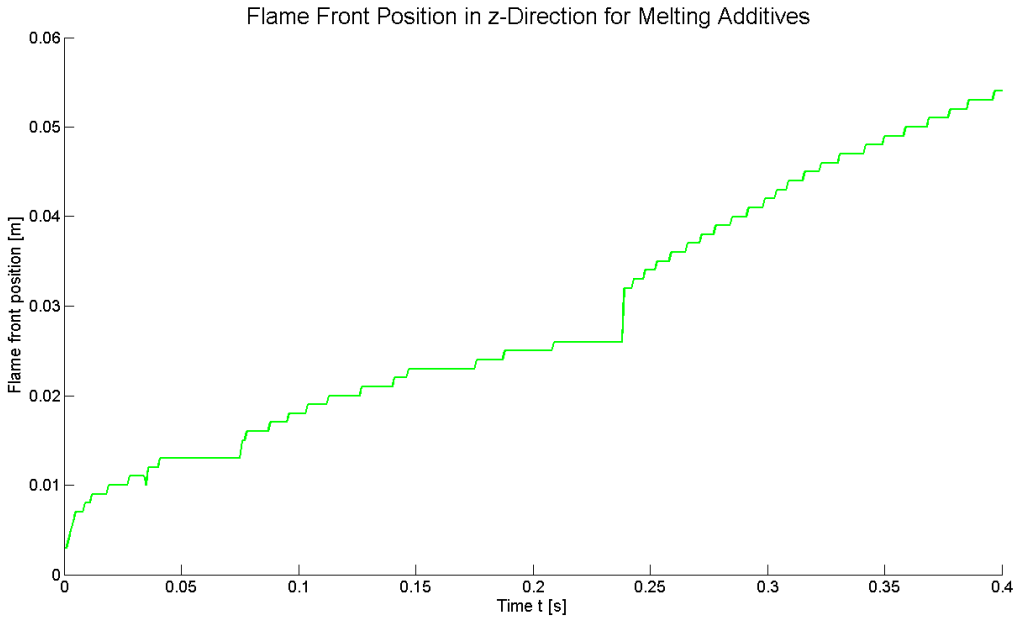

Figure 32: Flame front position over time for a Lycopodium/air mixture containing melting additives

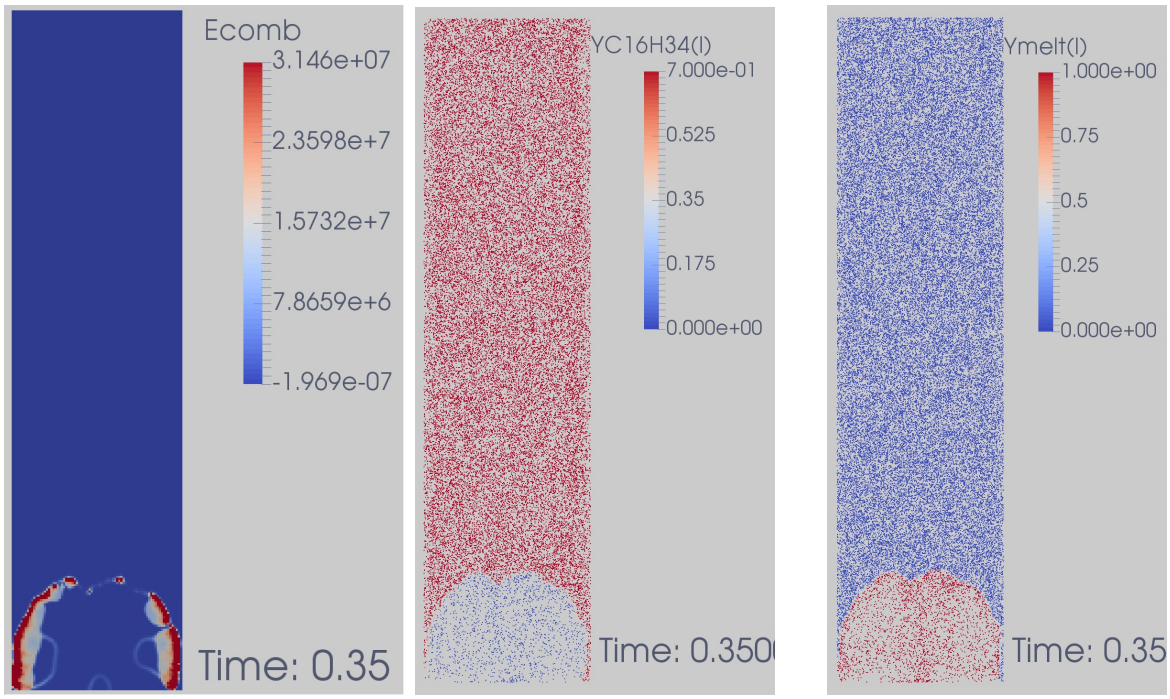

(a) Localisation of the flame front with vol. scalar field $Ecomb[J/m^3s]$

(b) $C_{16}H_{34}$-mass fraction $[-]$ in lycopodium particles

(c) Liquid mass fraction $Y_{melt}[-]$ in melting particles

Figure 33: Depiction of the flame propagation process on basis of three different quantities

Around $0.45\ s$ after ignition, streaks of slightly enhanced temperatures can be seen in the whole geometry. Another $0.1\ s$ later a hot zone separated from the flame front by an area of low temperatures appears and ignites spontaneously. The same happens to several small regions in the pipe. The combustion zones are growing very fast uniting until the whole geometry is affected.

Searching for the cause of this behaviour, one can observe that starting at around $0.39\ s$ the particles in the area above the hot zone are fused (figure 35). The melting takes place along streaks mainly over regions with maximum temperatures (dark red zones in table 7 column 4). Slowly, the affected area enlarges in terms of width and height. After $0.47\ s$ the first few particles above the flame front are completely molten. From that time on, one can observe a temperature increase in these cells where no melting is possible any more.

The types of heat transport that are decisively involved in this process are rather difficult to determine. On the one hand the advanced time would allow convection to play a role even with very low flow velocities on the other hand the local random formation of hot regions above the flame front would indicate radiation to be an important factor. Considering the behaviour of melting particles at the walls, two effects could be responsible for the less advanced phase transition in these regions. Firstly the walls have a cooling effect that has at least an influence on the temperature in the boundary layer. Secondly, due to the no-slip condition the velocity close

to the wall is small and convective heat transport therefore very low. Additionally the laminar base layer on the wall deteriorates the heat transfer from the gas phase to the particles.

Concerning radiation, its contribution to the above mentioned effect is difficult to be set on a specific value for reasons that have already been explained in 3.6. In [7] Proust states that radiation gains influence as a energy supply with growing flame thickness. This assumption fits together very well with the observations made within this thesis. Due to the very bad mixing conditions that are predominant in systems containing melting additives the oxygen remains unconverted in the back of the flame front. Through this the actual combustion zone stretches over a comparatively broad stripe (figure 33a in comparison with figure 29a).

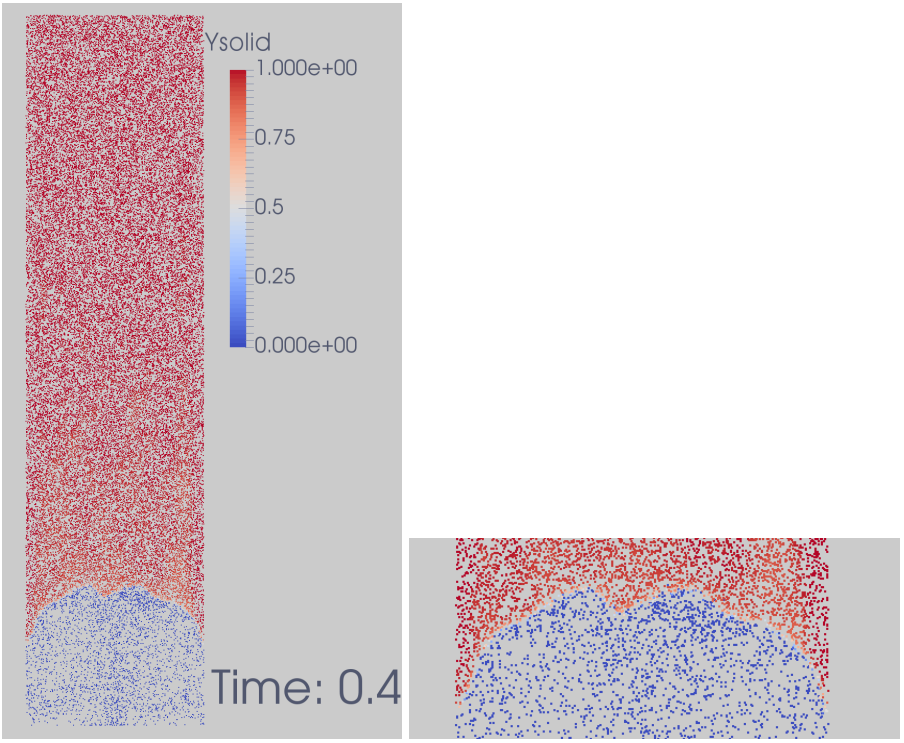

(a) Enlarged section

Figure 34: Melting progress (coloration with solid mass fraction $[-]$) for inert particles in lycopodium/air mixture at $t = 0.4\ s$

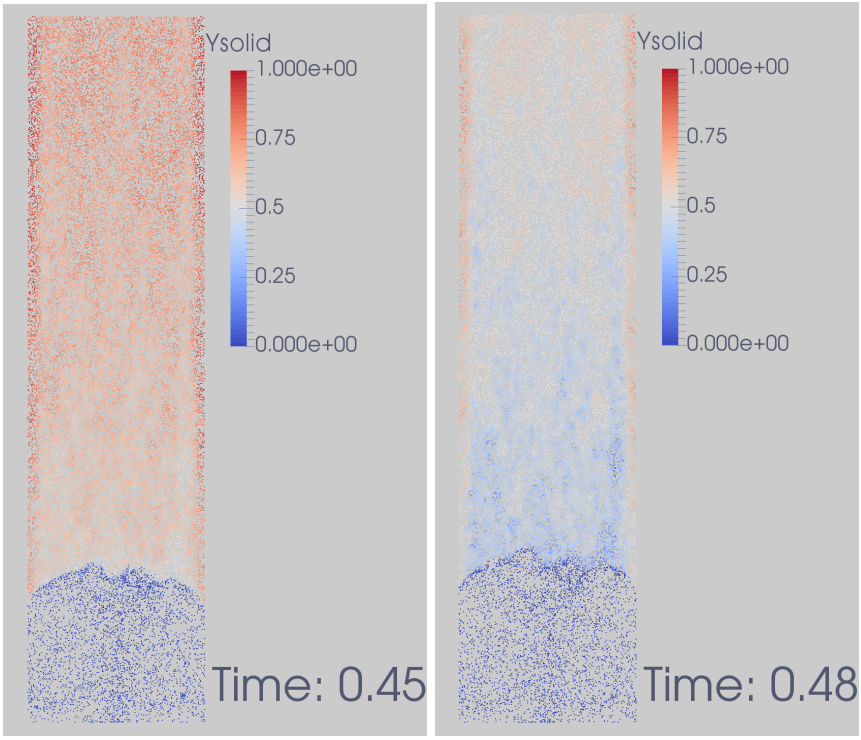

(a) Melting progress of inert particles

(b) Melting progress of inert particles

Figure 35: Melting progress of inert particles in lycopodium/air mixture at $t = 0.45\ s$ and $t = 0.48\ s$ (coloration with solid mass fraction)

8 Conclusion

The main objective of this thesis was to enlighten the interaction between particulate, inert additives and flammable dust/air-mixtures by means of CFD-modelling. Regarding several aspects of the flame-extinction/deceleration process this goal could successfully be accomplished. A general conclusion that could be derived from the carried out simulations is that the factors that control both investigated safety indices differ from each other. More precisely, a property that decreases the propagation velocity in a flammable heterogeneous mixture does not necessarily increase its Ignition Energy. In order to describe the behaviour of particulate extinguishing mediums it is important to determine more than one characteristic quantity. To get an integral view, the examination of two additional safety indices besides the already investigated ones would have been necessary, namely the pressure related quantities of Maximum Explosion Overpressure and the Maximum Rate of Pressure Rise.

Concerning the records of the energy source terms it was noticed that their content of relevant information was unfortunately lower than expected. The main problem was that for most terms energy absorption and release took place at the same time and the values cancelled each other. Only the combustion source term delivered useful data as it returns values of the same sign.

8.1 Water-Laden Particles

One major achievement of this study was to provide an explanation for the higher activity of certain systems containing water-laden additives that has been detected in experimental tests at the Chair of Thermal Processing Technology. The described tests were aimed to determine the Ignition Energy and were able to detect lower values for this type of system composition. However, they could not provide an explanation due to the limited availability of relevant measured quantities [22]. The general finding that the release of inert vapour or gas does not necessarily inhibit ignition and flame propagation is a very important aspect that has

to be considered in the development of extinguishing mediums. Effects as could be seen with water-laden particles should be prohibited by all means in order not to reinforce the negative consequences of dust explosions. The accelerated combustion and the additional water vapour that is released behind the flame front might for example even increase the pressure wave that comes along with the rapid reaction process.

Furthermore, it could be shown that the evaporation of water is thermally not competitive enough to deviate the available thermal energy from the combustion zone and is able to cool the mixture down only after the flame front has passed.

Summed up, water-laden particles show problematic behaviour in several manners and from the simulation point of view do not present themselves promising for real applications. Nevertheless, the simulations that were carried out within this thesis do not display the processes in real flame barriers and can therefore not give a clear statement on the performance under these conditions.

8.2 Melting Particles

As a complementation to the already possible modelling of simple inert particles and evaporating particles a completely new approach was implemented in OF that enabled to simulate the melting of particles. This type of additive is of special interest as it stands for many different extinguishing mediums that show any kind of heat absorption besides regular heat capacity without mass transport into the gas phase. The usage of this type of extinguishing mediums brings the advantage that the temporal and quantitative competitiveness compared to the combustion process can in contrast to water be regulated by the choice of material. Additionally no interaction with the gas phase in terms of mass transfer is taking place. In simulations the low activation energy for the process, in this case the heat of fusion, led to an early consumption of the available heat sinks in front of the flame. As a consequence hot regions that were spread over the whole geometry ignited spontaneously. In experimental tests at the Chair of Thermal Processing Technology similar experiences were made with this type of extinguishing medium. For mixtures that obviously ignited, no flame front could be tracked in the tube. It is possible that the effect that has been seen in the simulation leads to the problematic behaviour in experimental tests. As no measuring is possible in this case it is planned to gain more information about the real flame propagation by displaying this process via high speed camera.

Concerning the error that occurred in the simulation of melting particles regarding mass conservation it is purely physically not a problem to disable the mass transport from the Lagrangian to the Eulerian phase. However, it could be a problem for the correct CFD-modelling of the system as $OpenFOAM^{®}$ is obviously taking into account a kind of mass-specific interaction between the phases that should not exist. For now the submodel was used in spite of the occurred problem as it could be shown that the melting process is modelled physically correct

and deviations from the mass conservation in the gas phase could be kept low. However, for further usage of the melting particles even more effort has to be made to find the underlying reason(s).

8.3 Ignition Energy

The Ignition Energy turned out to be a very interesting index for displaying that the capacity of a heat sink is only one of several factors that control the extinguishing/suppressing performance of a particulate additive. Considering the results of this thesis it seems that specific thermal properties of a material come into effect only for the Flame Propagation Velocity and not for the necessary energy amount to ignite a flammable dust/air mixture. On basis of the gathered data it is also assumed that smaller particles show two beneficial effects that are able to improve their performance compared to the same concentration of bigger particles. Firstly they can follow the flow with less relative motion due to the small inertia that is inherent in them and can therefore remove more kinetic turbulent energy from the gas phase. This effect influences the turbulent diffusion that is necessary for good molecular mixing conditions and has a very short activation period compared to thermal mechanisms. Additionally, drag force reduces with decreasing diameters (surface) and leads to higher velocities of the particles in the flow. This in turn affects the heat transition by entering equation 5–15 through the heat transition coefficient α that considers velocity by means of the Reynolds number in the Ranz-Marshall correlation. Secondly the higher number of particles leads to a more homogeneous distribution in the geometry that increases the uniformity of the cooling effect and the overall particle surface for a better heat transition.

The basic model used for the simulations of the Ignition Energy was taken from Pollhammer [1]. In the course of this previously done work the general model was already evaluated in detail. Therefore at this point I refer to it for more information on this topic.

8.4 Flame Propagation

From [1] it was already known that the limiting step in the combustion region was clearly diffusion and hence the quality of micromixing. Considering the results of this thesis it is assumed that the inert particles affect the propagating combustion by controlling the two crucial processes of turbulent and molecular diffusion. As already discussed in 8.3 the impact that additives of the size of $50\ \mu m$ have on the Ignition Energy is rather low. In contrast, their influence on the flame propagation is very characteristic and causes specific velocity profiles for the proceeding combustions. It is assumed that the deviation that can be observed between the

behaviour of different systems is due to varying mechanisms that underlie their interaction with the combustion. Water-laden particles increase turbulence and thereby enhance the reaction rate of oleic acid.

Melting particles cool down the hot zone very fast and prohibit buoyancy effects caused by reaction products. Through this and through limiting the molecular diffusion due to lower temperatures they nearly stop the flame propagation in the pipe. The flame propagation velocity stays below $1\ m/s$ as long as solid material is available for melting. Although the combustion could not be extinguished the very slow reaction rates in the first stage of the combustion inhibit the development of a pressure wave that is the actual risk when dealing with dust explosions. Simple inert particles are less active than the previously mentioned additives both in terms of turbulence regulation and heat absorption.

The calculated flame propagation velocities would again be applicable for comparing simulation results with experimental data. As these values are very system specific they can only be compared to very similar experimental set-ups. Yet no data for this purpose is available but generally the determined velocities seem physically plausible.

9 Outlook

Within this thesis several aspects of the interaction between propagating dust explosions and inert particulate additives were detected. Some of them would have required more case studies or different approaches in order to be fully investigated. Due to the limited framework of the master thesis and the very time- and resource-consuming determination of Ignition Energies only a few effects could be observed in-depth. The others still provide enough scope for a more detailed examination. Besides the research perspectives the solver adaptations and newly introduced capabilities of Lagrangian particles can be used for many applications.

9.1 Outlook with Focus on Research Activity in the Field of Flame Extinction

Until now only one concentration level was investigated for both flammable dust and additives in the simulations of the ignition energy. From experimental work it is known that concentration has a strong impact on the behaviour of the system and would therefore be an interesting topic for further studies.

Concerning the relevance of radiation as a transport mechanism for released heat of combustion very little information is yet available. The impact of radiation is difficult to measure as all components in a system emit in all directions. The big advantage of simulations in this case is that specific physical processes can simply be switched off. By this means one could compare the results of a case where radiation is switched off with one where it is switched on and study the differences.

On basis of the additional scalar field $Ecomb$ that contains values for the released combustion energy it is possible to describe differences between the flame propagation behaviour also through the varying width of the reaction zone. Graphically the differences between the additives could already be recorded but tracking the $Ecomb$-peak described in 7.1 with a newer version of Matlab® would allow to write out its width over time which is basically a quantitative description

of the vertical length of the combustion zone. This value can also be determined experimentally with high-speed cameras and would be suitable for a comparison of results.

The primarily diffusion-limited reaction generally proposes that additives interfere with turbulent and/or molecular diffusion. For a better understanding of mechanisms underlying the interaction it would be of interest to examine to what extent both of them play a role in the suppressing process. Additionally to this the impact of turbulent kinetic energy absorption of inert particles could be observed also as a function of the particle diameter. In addition to the already considered extinguishing materials the existing approach that describes melting particles could be extended and modified so that it might simulate thermal decomposition or also a combined melting and vaporisation process. Moreover, it would basically be applicable for chemical interaction with the combustion process. However, the chemistry model that would be required for this purpose exceeded available computing performance easily and the time necessary for calculations would be several years.

Yet, no simulations were run displaying dust explosions under altering conditions such as increased/decreased pressure even though the capability of modelling those processes is the real strength of CFD. In cases where it is necessary to consider systems that are not reproducible in experimental tests, the numerical models can be used. This aspect for example becomes relevant if no experience is available for estimating the behaviour of specific materials or also extinguishing mediums under certain circumstances that alter from standard problems.

As already mentioned in a previous section, two safety indices are not enough to describe the behaviour of extinguishing materials in detail. Especially pressure related quantities would be of interest as the real destructive power of dust explosions stems from the development of pressure waves. In the observed geometries the pressure profile over time cannot be detected very well as the geometries are open to ambient pressure and the pressure compensation takes place very fast. In order to determine the Maximum Explosion Overpressure and the Maximum Rate of Pressure Rise Pollhammer [23] created a model similar to the experimentally used $20\ l$ SIWEK-apparatus. By using this geometry it would be possible to complete the studies on extinguishing materials.

9.2 Outlook with Focus on Application of the Results and the Implemented Simulation Features

The solver and the general case set-up are capable of simulations in bigger geometries. This means that besides the use in research also actual industrial applications can be modelled. Due to the feature OpenFOAM® provides for implementing injection cells into a geometry even extinguishing barriers are possible. In this context the timing of an injection and also its orientation and position would be an interesting topic for further investigations as well as the behaviour of suppressants when entering the geometry with high pressure. As it could be

observed within this thesis flame propagation can be strongly retarded by some additives leading to the occurrence of settling effects. Their influence on the propagating explosion would be interesting to investigate. Specific scenarios in models of existing plant sections and apparatuses could also be simulated.

Due to the fact that only fundamental mechanisms were observed within this study only very little afford was placed on the choice of material properties. As OpenFOAM® allows the user to change existing materials and create their own ones, cases could be run focussing on very material specific behaviour. Also comparisons between different extinguishing powders would theoretically be possible.

References

[1] Pollhammer, W., Numerische Untersuchung der Mindestzündenergie sowie der Flammenfortpflanzung in Staub/Luft - Gemischen mittels eines Euler - Lagrange - Modells in OpenFOAM, Montanuniversität, 2015.

[2] U.S. Chemical Safety and Hazard Investigation Board, Investigation Report - Combustible Dust Hazard Study, (2006), Retrieved from `http://www.csb.gov/assets/1/19/dust_final_report_website_11-17-06.pdf` 27-8-2016.

[3] Bartknecht, W., Staubexplosionen: Ablauf und Schutzmaßnahmen, Springer Verlag, Berlin-Heidelberg-New York, 1987.

[4] Bartsch, C. and U. Schubert, Praktikum Sicherheitstechnik: Versuch 1 - Modifiziertes Hartmannrohr, lecture notes, HS Merseburg, Retrieved from `http://web.hs-merseburg.de/~ag-vt/HMR_VA.pdf` 27-7-2016.

[5] Eckhoff, R. K., Explosion hazards in the process industries, Gulf Pub, Houston TX, 2005.

[6] Dobashi, R., Flame propagation during dust explosions, Proceedings of the 5th International Seminar on Fire and Explosion Hazards, Edinburgh, UK, (2007), Vol. 23 p.27

[7] Proust, Ch., A few fundamental aspects about ignition and flame propagation, Journal of Loss Prevention in the Process Industries 19 (2006), 2-3, p. 104-120.

[8] Chen, J.L., R. Dobashi and T.Hirano, Mechanisms of flame propagation through combustible particle clouds, Journal of Loss Prevention in the Process Industries 9 (1996), 3, p. 225-229.

[9] Cote, A.E., Operation of fire protection systems - A special edition of the Fire Protection Handbook, National Fire Protection Association, Quincy Mass, 2003.

[10] Krasnyansky, M., Studies of fundamental physical–chemical mechanisms and processes of flame extinguishing by powder aerosols, Fire Mater. (Fire and Materials) 32 (2008), 1, p. 27-47.

[11] Hurley, M.J. (Editor in Chief), SFPE Handbook of Fire Protection Engineering, 5th edition, Springer, New York, 2016.

[12] Warnatz, J, U. Maas, R.W. Dibble, Verbrennung, Springer Verlag, Berlin Heidelberg, 2001.

[13] Fluent Inc. (publisher), Fluent 6.0 User's Guide, Volume 4, Chapter 18 - Introduction to Modelling Multiphase Flows, Lebanon NH, USA, (2001), p. 1-5, Retrieved from http://www.afs.enea.it/fluent/Public/Fluent-Doc/PDF/chp18.pdf 01-08-2016.

[14] Bakker, A., 14. Multiphase Flow, Lecture Notes, Dartmouth College, 2006, Retrieved from: http://www.bakker.org/dartmouth06/engs150/ 1-8-2016.

[15] Davidson, L., An Introduction to turbulence models, Chalmers University of Technology, (2015), Retrieved from: http://www.tfd.chalmers.se/~lada/postscript_files/kompendium_turb.pdf 06-09-2016.

[16] Paul, E.L., Handbook of Industrial Mixing - Science and Practice, Wiley Interscience, Hoboken NJ, 2004.

[17] Brennen, C. E., Fundamentals of multiphase flow, Cambridge Univ. Press, Cambridge MA, 2006, Retrieved from: http://authors.library.caltech.edu/25021/2/cabook.pdf 09-09-2016.

[18] Greifzu, F., C. Kratzsch, T. Forgber, F. Lindner, R. Schwarze, Assessment of particle-tracking models for dispersed particle-laden flows implemented in OpenFOAM and ANSYS FLUENT, Engineering Applications of Computational Fluid Mechanics 10 (2015), 1, p. 30-43.

[19] http://www.openfoam.com/, 06-08-2016.

[20] Energy equation in OpenFoam, http://cfd.direct/openfoam/energy-equation/, 08-08-2016.

[21] Zuo, B., A.M. Gomes, C.J. Rutland, Studies of Superheated Fuel Spray Structures and Vaporization in GDI engines, International Journal of Engine Research 1 (2000), 4, p. 321-336.

[22] Hüttenbrenner, K., C. Donner, H. Kern and H. Raupenstrauch, Investigations on the influence of the specific surface on the ignition and flame behavior of combustible dust/air-mixtures, 11th International Symposium on Hazards, Prevention, and Mitigation of Industrial Explosion (ISHPMIE), Dalian, CN, (2016)

[23] Pollhammer, W., Entwicklung eines alternativen Staubverteilungssystems für die 20 Liter SIWEK - Apparatur mittels CFD-Methoden, Montanuniversität, 2015.